MICROCLIMATE AND PHENOLOGY AT THE H.J. ANDREWS EXPERIMENTAL FOREST

by

SARAH E. WARD

A THESIS

Presented to the Department of Biology
and the Graduate School of the University of Oregon
in partial fulfillment of the requirements
for the degree of
Master of Science

March 2018

THESIS APPROVAL PAGE

Student: Sarah E. Ward

Title: Microclimate and Phenology at the H.J. Andrews Experimental Forest

This thesis has been accepted and approved in partial fulfillment of the requirements for the Master of Science degree in the Department of Biology by:

Bitty Roy	Chairperson
Dan Gavin	Member
Mark Schulze	Member

and

Sara D. Hodges	Interim Vice Provost and Dean of the Graduate School

Original approval signatures are on file with the University of Oregon Graduate School.

Degree awarded March 2018

THESIS ABSTRACT

Sarah E. Ward

Master of Science

Department of Biology

March 2018

Title: Microclimate and Phenology at the H.J. Andrews Experimental Forest

Spring plant phenology is often used as an indicator of a community response to climate change. Remote data and low-resolution climate models are typically used to predict phenology across a landscape; however, this tends to miss the nuances of microclimate, especially in a mountainous area with heterogeneous topography. I investigated how inter-annual variability in regional climate affects the distribution of microclimates (i.e., areas <100m^2) and spring plant phenology across a 6400-hectare watershed within the Western Cascades in Oregon. Additionally, I created species-specific models of bud break at the microclimate scale, that could then be applied across a wider landscape. I found that years with warm winters, few storms and low snowpack have a homogenizing effect on microclimate and spring phenology events, and that bud break models developed at a local scale can be effectively applied across a broader landscape.

This thesis includes previously unpublished coauthored material.

CURRICULUM VITAE

NAME OF AUTHOR: Sarah E. Ward

GRADUATE AND UNDERGRADUATE SCHOOLS ATTENDED:

University of Oregon, Eugene
Michigan State University, East Lansing

DEGREES AWARDED:

Master of Science, Biology, 2018, University of Oregon
Bachelors of Science, Wildlife Management and Biology, 2012, Michigan State University

AREAS OF SPECIAL INTEREST:

Forest Ecology

PROFESSIONAL EXPERIENCE:

Forestry Research Technician, Oregon State University, 2012-2018

Graduate Teaching Assistant, Department of Biology, University of Oregon 2016-2018

Graduate Teaching Assistant, Department of Geography, University of Oregon 2016-2017

GRANTS, AWARDS, AND HONORS:

Travel Grant, Ecological Society of America, 2017

PUBLICATIONS:

Ward, S., Schulze, M., & Roy, B. (in review). A long-term perspective on microclimate and spring plant phenology in the Western Cascades. *Ecosphere.*

ACKNOWLEDGMENTS

Many thanks to Mark Schulze, Bitty Roy and Dan Gavin for their assistance in both the research and writing aspects of this thesis. This work was funded by the NSF LTER program (DEB 1440409). Data and facilities were provided by the HJ Andrews Experimental Forest and Long Term Ecological Research program, administered cooperatively by the USDA Forest Service Pacific Northwest Research Station, Oregon State University, and the Willamette National Forest. Special thanks to Jay Sexton and all of the people who assisted with data collection in one or more seasons. And last but not least, many thanks to Rob Miron and Jessica Celis for the moral support.

TABLE OF CONTENTS

Chapter Page

LIST OF FIGURES

LIST OF TABLES

Table Page

CHAPTER I

INTRODUCTION

Phenology – the study of recurring seasonal life cycle events – is a simple metric that can be used to elucidate patterns among communities and across ecosystems. Plant phenology is easily observable and can be measured by citizens and scientists alike. Regional climates across the globe have been steadily increasing in temperature (IPCC 2014), and as temperatures continue to warm, the timing of annual leaf emergence and flowering has advanced as much as 2 to 3 days per decade (Parmesan and Yohe 2003, Menzel et al. 2006). These advancements can have sweeping impacts beyond a single trophic level, and can reduce the fitness of plants, animals and insects within a community (Walther et al. 2002, Parmesan and Yohe 2003, Both et al. 2009, Thackeray et al. 2016) Local climates (areas <100m^2) driven by variable topographies, canopy cover and temperature inversions have been shown to buffer temperature advances and in turn have the potential to minimize advanced phenological events (Daly et al. 2010, Dobrowski 2011, Pepin et al. 2011, Frey et al. 2016b, Novick et al. 2016, Lenoir et al. 2017). I investigated the effects of regional climate patterns on the distribution of microclimates in a 6400-hectare watershed in the Western Cascades, and in turn, how those microclimates affect the spring plant phenology of 18 native species of herbs, shrubs and trees. Because each species has evolved a unique physiological response to climate (Kreyling 2010), I was interested in creating species-specific models to predict bud break using local temperature metrics. Most predicted effects of regional warming are derived using low resolution spatial models and then downscaled to higher spatial resolutions. This method misses the nuances of local microclimates and can over or under predict the effects of regional change on a community. By creating local scale models at high spatial resolution that can then be applied to a wider region, I hoped to remove this source of error, and create models that can accurately predict bud break across a landscape.

Chapters II and IV of this thesis are both co-authored material and will be published with Bitty Roy and Mark Schulze listed as co-authors. Chapters I, III and V are all sole authored by Sarah Ward.

CHAPTER II

A LONG TERM PERSPECTIVE OF MICROCLIMATE AND SPRING PLANT PHENOLOGY IN THE WESTERN CASCADES

Acknowledgements

This chapter includes materials currently under review and co-authored by Sarah Ward, Mark Schulze, Bitty Roy.

Introduction

Over the past several decades, scientists and land managers have become increasingly concerned about the effects of current warming trends and the potential threat warming poses to biodiversity and ecosystem services (Grimm et al. 2016). Phenology – the timing of seasonal events of an organism's life cycle – is a common measure of the response of a species to climate change, and phenological shifts can have significant impacts on the dynamics of an ecosystem (Walther et al. 2002, Parmesan 2006, Both et al. 2009). For example, because not every species responds equally to changes in climate, trophic levels with historically synced phenologies, such as plants and pollinators, may become decoupled due a shift in one or both species' phenologies (trophic asynchrony), and result in localized population declines and biodiversity loss (Harrington et al. 1999, Walther et al. 2002, Visser et al. 2004, Visser and Both 2005, Parmesan 2006, Inouye 2008, Both et al. 2009, Forrest and Thomson 2011, Thackeray et al. 2016). Parmesan and Yohe (2003) reviewed data time series data on the phenology of 677 species for periods spanning from 16-132 years in length (median 45 years) and found that 62% of those species had shown some change in their phenologies, and that 87% of phenological shifts were in the direction expected due to climate change. For plants, they found that spring events such as bud break (first date of leaf emergence) and flowering are advancing at an average rate of 2.3 days per decade.

Models developed to predict the effects of climate warming on biodiversity are often based on regional climate projections, which are too coarse (>50km^2) to predict the variation in local climate (microclimate) that organisms experience (Peterson et al. 1997, Lookingbill and Urban 2003, Luoto and Heikkinen 2008, Daly et al. 2010, Pepin et al.

2011, Potter et al. 2013, Frey et al. 2016b). Physical factors such as topography, snowpack accumulation and ablation, and forest cover can have significant effects on local climate, and in turn affect the timing of phenological events (Hwang et al. 2011). These microclimates can be significantly different from regional climate patterns and downscaling regional models may result in overgeneralization when projecting the effects of climate change (Daly et al. 2010, Franklin et al. 2013, Frenne et al. 2013) Mountainous regions—which make up 12.3% of the terrestrial surface on earth, excepting Antarctica (Körner et al. 2011)—are especially overgeneralized in regional models, due to the high degree of topographic heterogeneity (Luoto and Heikkinen 2008). Additionally, climate stations are often biased towards lower elevation, accessible sites, resulting in higher incidences of estimated data for remote upper elevation sites (Pepin et al. 2011). Steep mountainous terrain often leads to persistent cold air pooling events (temperature inversions) where cold air drains down mountain slopes into valleys and other areas of low topographic relief and is trapped by a layer of warmer air above and the local climate is decoupled from the regional atmospheric conditions. These events are a major driver of microclimate in mountainous regions, especially during winter months and they are largely driven regional weather patterns (Daly et al. 2010, Pepin et al. 2011, Novick et al. 2016). Some studies suggest that microclimates created by topography, canopy cover and local decoupling from regional weather patterns may mitigate the effects of regional warming, and have the potential to buffer temperatures and minimize advanced phenological events (Peterson et al. 1997, Daly et al. 2010, Dobrowski 2011, Frey et al. 2016b, Lenoir et al. 2017)

Here we report results of an eight-year study involving weekly spring phenology observations of 18 species of plants across a diverse range of fixed sites in the H.J. Andrews experimental forest on the west slope of the Oregon Cascades. We were interested in how microclimates vary across a watershed, and how regional climate variability and microclimate processes interact to influence the timing of spring phenology of native herbs, shrubs, and trees. In general, we expected that warm years with less snow pack would result in advancement of bud break and flowering, especially for the higher elevation, exposed ridgelines, and vice versa for cooler years with deeper and more persistent snowpack. Specifically, we expected to see the effects of cold air

pooling across the landscape reflected in the timing of phenology in two ways. First, we hypothesized that areas more susceptible to cold air pooling would experience less early-season temperature forcing and more persistent snowpack than topographically exposed sites of similar elevation, which would be reflected in relatively delayed spring phenology of forest plants. Second, we expected that interactions between regional and local processes may result in year to year variability in the relationship among sites across the elevation gradient (e.g., the timing bud break may be similar at two sites one year, and be widely different between those sites a different year).

Methods

Study area

The H.J. Andrews Experimental Forest is a 6400-hectare (15,800 acre) forest located on the west side of the Cascade Mountains around 50 miles east of Eugene, Oregon. The area is typical of the Western Cascade Range, with steep mountainous terrain, exposed ridges and sheltered valleys, and a high degree of topographic heterogeneity with elevations ranging from 410 to 1630 m. Vegetation is primarily a combination of 150-500 year old mixed conifer forests, and 40-60 year old *Pseudotsuga menziesii* (Douglas fir*)* plantations.

Study design

6" Sixteen core phenology sites were selected across a variety of elevations and aspects, with sites ranging from 460 to 1339 meters (Figure 1). Most phenology sites were co-located (11 of 16 sites) with long term temperature (Johnson and Gregory 2016, Daly and McKee 2016a, 2016b) and vegetation monitoring plots (Harmon and O'Connell 2015, Franklin 2017). This allowed for quality assurance and quality control (QAQC), and data validation using comparable temperature data. Additional sites (beyond those 11 co-located with long term monitoring plots) were added to augment distribution of study sites across elevation, aspect and topographic position and to create old growth and plantation paired sites at high, medium and low elevations. 18 species of native herbs, shrubs and trees were selected as target species (Appendix S1: Table S1). At each site, a center point was established and plants from all of the focal study species occurring in the area (due to the variety of terrain and elevation, not every target species was found at

every site) were added as encountered while inventorying a 25m radius circle around the center point until 5 individuals of each species were mapped and tagged (in the 2009 pilot season, only 3 individuals per species were tagged, the sample sizes were increased to 5 early in the 2010 season). In a few instances, plants of a given species were tagged up to 35m away from the center point to attain the target sample size. Each plant was mapped using bearing and distance from the center post. For herbaceous plants, individuals were marked using one or two pin flags with a numbered aluminum tag attached to the pin flag. Trees and shrubs were tagged using aluminum nails or zip ties depending on stem

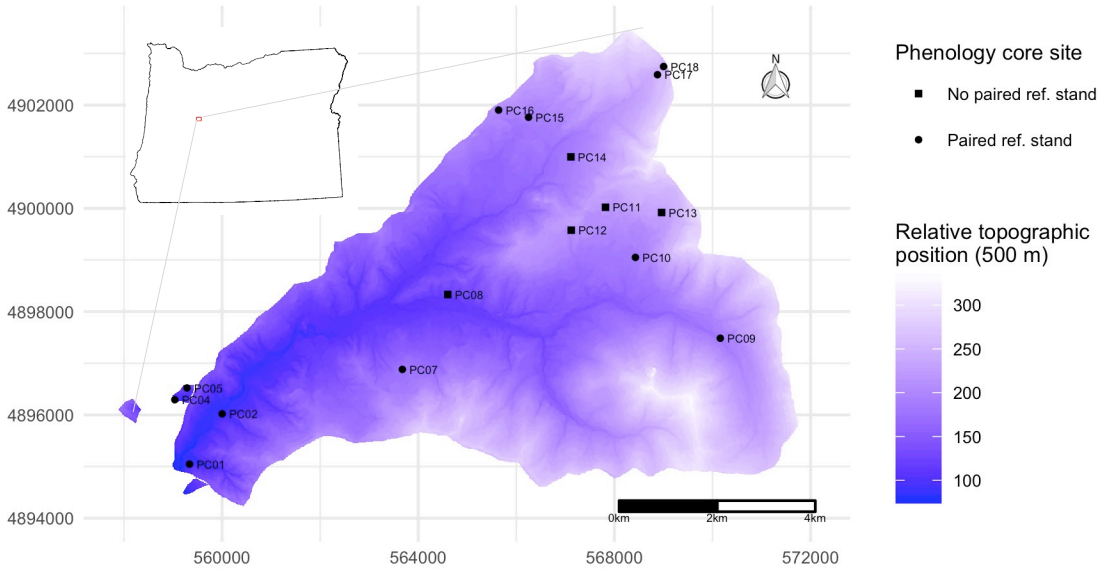

Figure 1: Map showing the location and relative topographic position of the 16 core phenology sites at the H.J. Andrews. Colors are relative topographic position, with blues showing sites of low topographic relief, and whites showing sites with high topographic relief. Purples are intermediate values. Squares indicate sites without a paired reference stand, while circles are sites with a nearby reference stand. Sites are labeled with PC (phenology core) and the site number.

diameter. If an individual died or was eaten over the course of the study, another plant was selected to maintain five individuals per site.

Understory air temperature and snow cover were the primary microclimate variables recorded. To capture the temperature of each site, HOBO (Onset Corporation, Hobo U22-001; accuracy 0.2°C) temperature sensors were placed 1.5 meters above the ground facing south in the center of each plot, and temperature data were collected every fifteen minutes. To reduce temperature spikes due to solar radiation, the sensors were placed in the shade, beneath a PVC shield (a 20.32cm long piece of 7.62 cm schedule 40 pipe split in half lengthwise). Snow data were collected via observations of depth and

percent cover made by researchers during each site visit, and partial or full burial under snow was recorded for each individual. Snow data for the winter period prior to the first phenology census were estimated using existing snow stake datasets (Schulze and Levno 2017), Andrews meteorological stations (Daly and McKee 2016b), time lapse cameras distributed across the forest, and observations from other researchers.

Surveys

We developed a species-specific scoring system for vegetative and reproductive phenophases that captured consistently observable stages between dormant buds and full leaf out/end of flowering (Schulze 2017). Over the course of each spring, the sites were visited once every 5-10 days, and each individual was scored based on its current reproductive and vegetative phenophase. In the early years of the study (2009 and 2010), visits were less consistent, due to concurrent study plot set up and early season site access limitations. From 2011-2016, sites were typically visited once every 7 days. Observations began each year in late winter with the start date varying depending on observed winter weather, snow pack and plant condition across the elevation gradient, with the goal of initiating observations at each site prior to the onset of key phenophases (e.g., bud swell) of focal plant species. In 2015, only a subset of seven sites were visited due to budget and time limitations. To reduce bias in cross-site comparisons due to observations occurring on different days of the week (it was generally not logistically feasible to visit all sites on the same day, but visits were scheduled to occur within a one to four-day window), all observation dates were standardized to the midpoint of each week. Weeks were defined as day of year weeks rather than based on the calendar of each year, meaning regardless of what day (i.e., Monday, Tuesday) the year began on, the mid-point of the first week of the year is day of year 3, and the mid-point of week two is day of year 10. Occasionally, individuals would exhibit significant development over the course of a week, resulting in missed scores for particular phenophases. For example, a plant may be observed at bud swell one week, and have emerging leaves the subsequent week, with bud break occurring sometime in the interim. In such cases, we estimated these missed scores by splitting the difference between each observation (e.g., if bud swell was observed on day of year 30 and emerging leaves were observed on day of year 37, we interpolated that bud break occurred on day of year 33). No attempt was made to

estimate the timing of phenophases that occurred prior to the first visit of each year, or after the last summer visit.

Data processing

QAQC was conducted on all temperature data collected. All data were averaged into hourly segments and run through python (Frey et al. 2016b, Johnson and Hadley 2017) to identify and flag impossible values, periods of missing data, and when sensors were buried by snow. We then further checked the data via manual QAQC and compared values to those from nearby temperature stations to identify any erroneous snow flags (i.e. data flagged as snow burial when there was no snow at that site), as well as temperature spikes, missing data, and other questionable values not identified by automated QAQC. To produce cumulative measures of temperature forcing, all data flagged for removal (sensor error, impossible values, missing data, snow burial), were filled via regressions using nearby long-term temperature stations (Daly and McKee 2016a, 2016b) (Appendix S1: Table S2). All regressions used to interpolate temperature data had an adjusted R^2 of 0.97 or greater, and most (11 of 16) came from stations 25-200 m from the phenology plot. Growing degree days were calculated by summing all degree hours greater than 5° C accumulated over a 24-hour period and dividing that sum by 24 to get the average daily accumulation of growing degree days for a given microclimate (Murray et al. 1989, Heide 1993). Starting from December 1, we added each subsequent daily accumulation of degree days. This allowed us to estimate the total growing degree days accumulated on April 1 as an indicator of winter and spring temperature forcing. We also used the winter anticyclonic-cyclonic index (A-C index) developed by Daly et al. (2010 and unpublished) as an indicator of year to year variability in regional winter (Dec 1 – Mar 31) weather patterns. This index, calculated by subtracting the number of cyclonic (stormy/low pressure) days from the anticyclonic (clear/high pressure) days, has been shown to correlate strongly with patterns of cold air pooling and temperature inversions using methods described by Daly et al. (2010). We used data from two permanent meteorological stations on the Andrews to compare temperatures at high elevations (out of temperature inversions) and low elevations (typically beneath winter temperature inversions) to confirm the presence of winter cold air pooling events. Our assumption was that cold air pools were likely present if the lower elevation sites

deviated from normal at a lesser rate than higher elevation sites, meaning that the lower sites had temperatures that were decoupled from the regional conditions while the higher sites were not.

Analysis

Data analysis was conducted using R statistical software (version 3.3.2) and R studio (version 1.0.153) (Appendix S3). For microclimate analysis, we compared local and regional climate with a variety of temperature and climate metrics. We created linear models to regress elevation against bud break and flowering; the assumptions of linear models were checked for each model, and data were transformed where necessary to meet assumptions of normality. Additionally, collinear temperature variables (Appendix S1: Table S3) were condensed using principle components analysis (PCA) to compare microclimates between years and across sites; all assumptions of a PCA were tested.

Results

Microclimate

From 2009 to 2016, there was a large amount inter-annual variability both within and across sites. To see how the climate during phenology years compared to other years at the Andrews, we looked at temperature data from two historic reference stands with contrasting elevations and topographic positions (RS02, 478m and RS04,1300m) associated with phenology sites. We found that from 1970 until 2015, growing degree days (GDD) accumulated between December 1 and March 31 (hereafter, winter) fluctuated greatly between years (Figure 2a), as did the winter A-C index (Figure 2b). 1982 had the lowest A-C index (-7) and the winter GDD at both the high and low elevation sites is nearly 0, with little difference between the two sites. In contrast, 2015 had an A-C index of 44 and growing degree days at both sites are well above 100. That year, RS04 (the high elevation site) accumulated more GDD than any other year in the 46-year record. Data from all 16 phenology sites over the course of this study also showed this strong inter-annual variation in climate (Figure 3a, Appendix S1: Table S4, S5).

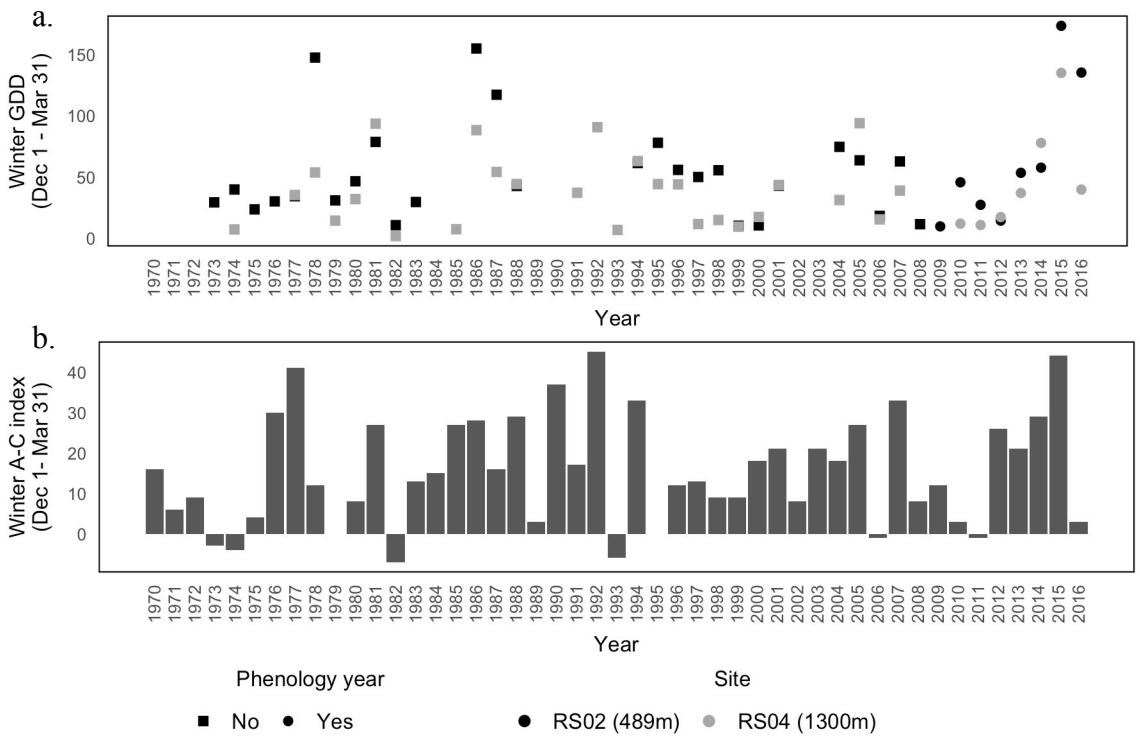

Figure 2: Historic winter climate at high and low elevation sites at the H.J. Andrews. (a) Winter A-C index values for the entire Andrews watershed from 1970 until 2016. (b) Winter growing degree days between 1970 - 2016 from two reference stands at the H.J. Andrews. In figure (a), squares indicate years without phenology surveys, and circles indicate years included in the phenology dataset. For both figures, grey indicates data from reference stand 2 (RS02), which is located at 489 m in an old-growth forest. Black indicates data from reference stand 4 (RS04), which also located in an old-growth stand, but at 1300 m. Years with incomplete data were not included in either figure.

To confirm the presence of winter temperature inversions, we compared data from two permanent meteorological stations (PRIMET 436m, UPLO 1284 m) to the 30 year average (179 – 2008), and found that years with lower AC indices (2010, 2011, 2016) tended to have winter temperatures that deviated similarly from normal at both high and low elevation sites (Figure 3b). In 2011 and 2016 (low AC indices), the high elevation site deviated only 0.35 and 0.35 more from normal than the low elevation site. In 2014 and 2015 (high AC indices), the mean winter temperature at the high elevation site deviated 0.07 and 3.35 degrees above normal while the low elevation site was 0.8 degrees below normal in 2014 and 2.1 degrees above normal in 2015 (a difference of 0.87 and 1.25 between high and low sites). This is likely due to cold air pooling events buffering temperatures low elevation sites during years with high AC indices. Sites with high

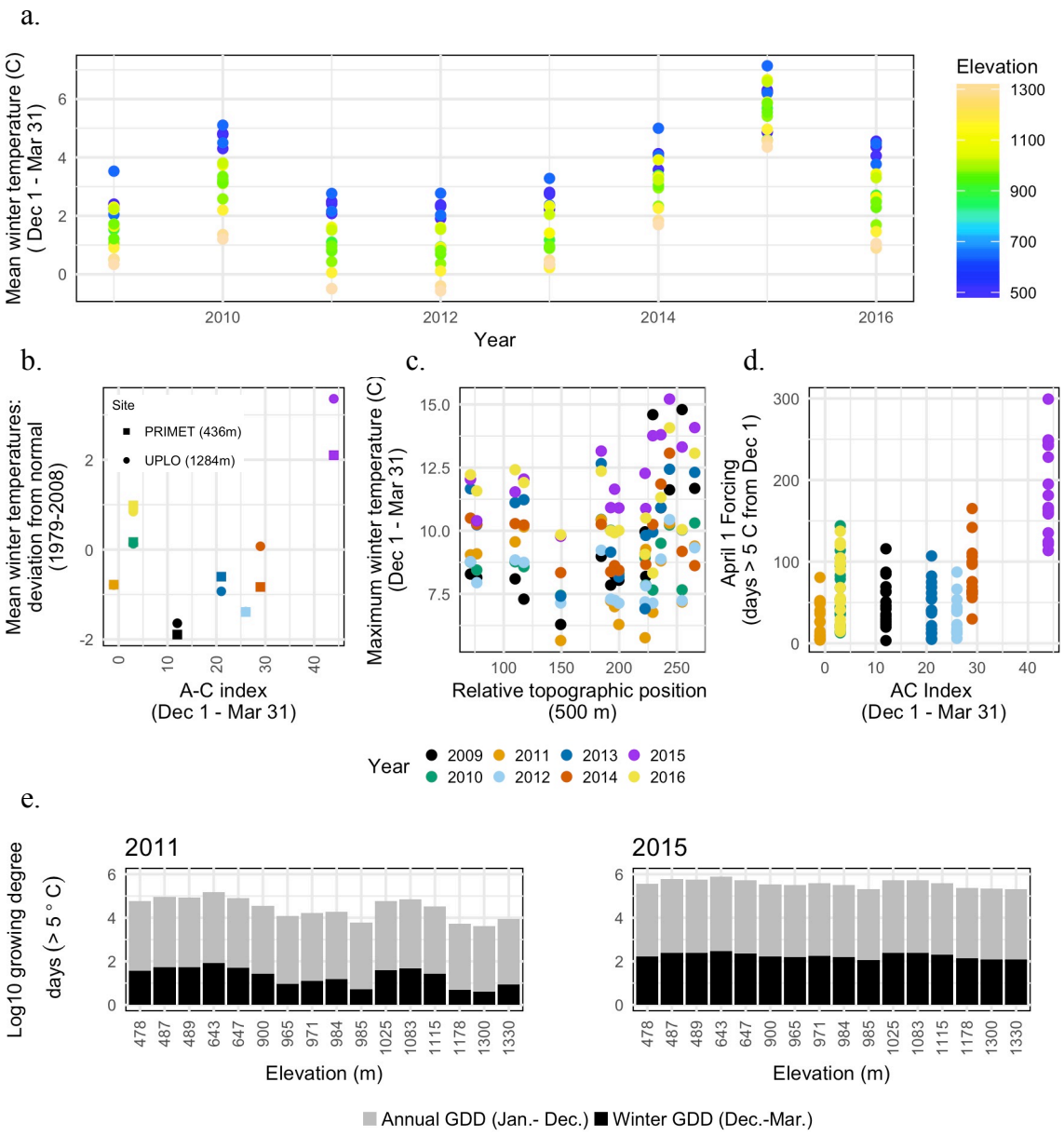

Figure 3: Microclimate patterns between 2009-2016. (a) Mean winter temperatures at all sites. Colors represent elevation, with low elevation sites in blue, high elevation sites in yellow. Intermediate elevations are in green. **(b) Difference from the 30-year average (1979-2008) of mean winter temperatures at two permanent meteorological station at the HJA relative to the winter AC index.** PRIMET is a station near the Andrews headquarters and is at 436 meters; it is represented by filled squares. UPLO is a high elevation site at 1284 meters and is represented by circles. **(c) Maximum winter temperature relative to topographic position.** Colors represent year while each point is a site during a given year. **(d) GDD accumulated on April 1 at each site relative to the winter AC index.** Colors are different years, while each colored point represents a different site during a given year. **e.) Winter and annual GDD at all sites in 2011 and 2015.** Grey bars are GDD accumulated between January 1 and December 31 at each site, while black bars are GDD accumulated between December 1 and March 31 at each site.

relative topographic position also saw greater variability in maximum winter temperature than sites with low topographic position (Figure 3c), another indicator that cold air pooling buffered winter temperatures from regional warming. In the eight years when phenology surveys occurred, 2011 and 2015 represent the coolest and warmest years respectively. We used a two tailed, unpaired t-test to compare 2011 and 2015 conditions and found that in 2015 all sites accumulated significantly more growing degree days by April 1 ($p<0.001$, $t = -10.62_{(df=19.865)}$) than in years with a lower A-C index like 2011 and there was less difference in winter growing degree day accumulation between high and low elevation sites in 2015 compared to 2011 (Figure 3d). In 2015, sites 500 meters apart in elevation accumulated the same amount of growing degree days (242.6 and 242.7) between Dec 1 and Mar 31.

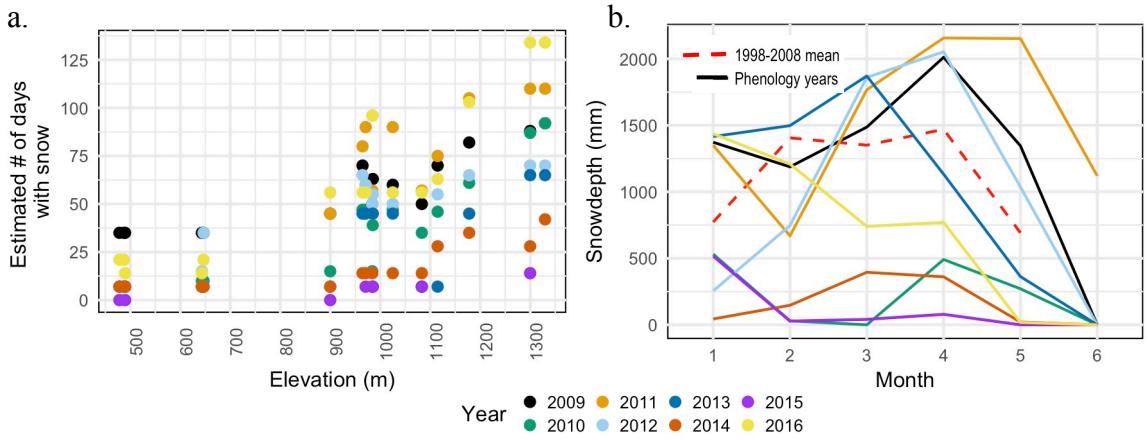

Figure 4: Snow depth during the phenology years. (a) Estimated number of days of snow at each phenology site in a given year. Data was estimated using observations and nearby meteorological stations and snow stakes. Colors represent years, while each point is a site in a given year. **(b) Snow depth at a high elevation meteorological station (VANMET, 1285 m) on the first of each month between January and June**. The red dashed line is the 10-year average from 1998 to 2008, and the solid lines are phenology years. Colors are different years.

Snow was highly varaible across all year (Figure 4). In 2015, most precipitation fell as rain, resulting in minimal snowpack even at the highest elevations on the Andrews (Sproles et al. 2017). In 2011, snow persisted well into June at the 1284 m meteorological station, while all of the other years had little to no snow by June 1. The first date where 0% of plants were buried under snow was on average 94 days earlier in 2015 than 2011 (Appendix S1: Table S6). One mid-elevation site (PC15, 971m) had all plants exposed at least 144 days earlier in 2015 than in 2011.

Finally, we used a principle components analysis to compare collinear temperature variables (Figure 5). The first two principle components of the microclimate PCA explained 73.3% of the variance in microclimates between sites and years. The first principle component explained 63.0% of the variation among sites and years, and primarily separated sites by mean seasonal (Fall: Oct-Dec, winter: Jan-Mar, spring: Apr-Jun and summer: Jul-Sept) mean annual (November 1 to October 31) temperature and April 1 GDD (from Dec 1). The second principle component explained 10.3% of the variance between site microclimates, and primarily separated sites by fall average (89.4% of the axis). We used best subsets to select a model using physical variables to predict principle component 1 (Appendix S1: Table S9), and were able to predict 73.1% of the variance in PC1 using aspect, slope, elevation, topographic index and winter AC index ($F_{(5,122)}$= 66.39, p<2.2e-16). Winter AC index alone explained 23.3% of the variance ($F_{(1,126)}$38.19, p = 8.2e-9) and elevation explained 38.3% of the variance in PC1 ($F_{(1,126)}$78.24, p = 6.9e-15).

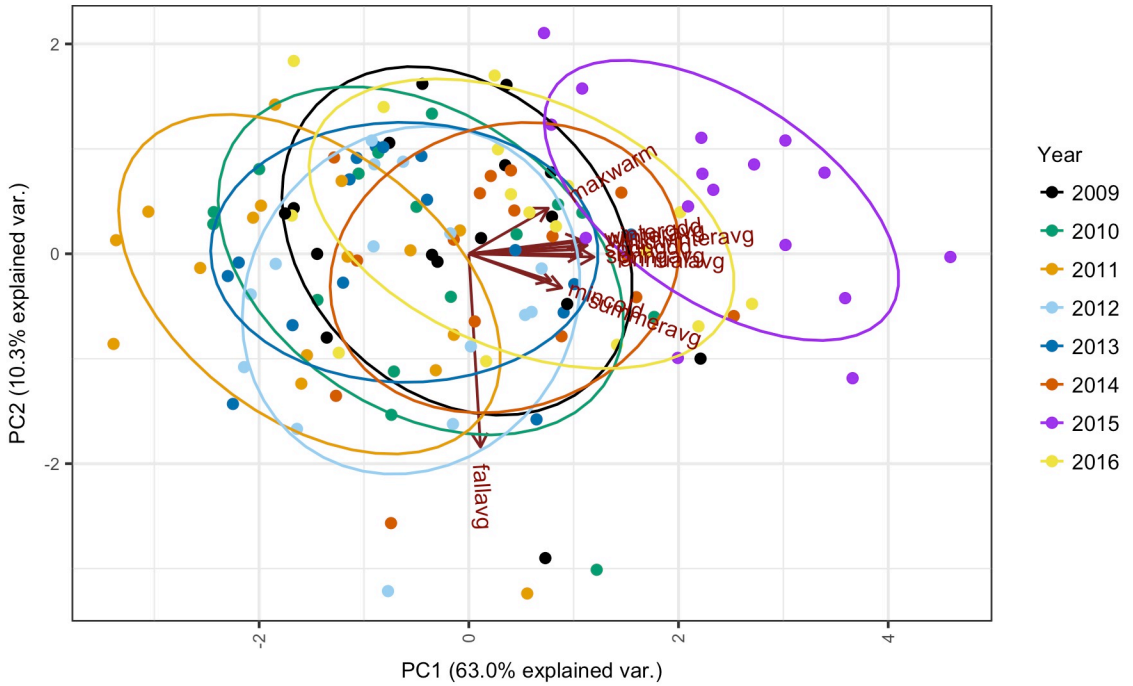

Figure 5: A principle components analysis of temperature variables at all 16 sites between 2009 and 2016. Ellipses represent 95% confidence intervals. Colors represent years and each point is a site during a given year.

Phenology

Plant phenology generally tracked the inter-annual variability of microclimates, although individual species varied in their responses to microclimate differences. The general pattern of relatively early bud break in warm years and late bud break in cold years was consistent across all focal species and sites (Figure 6; Appendix S1: Fig S1). We saw a loss of diversity in the timing of bud break in years with a higher AC index

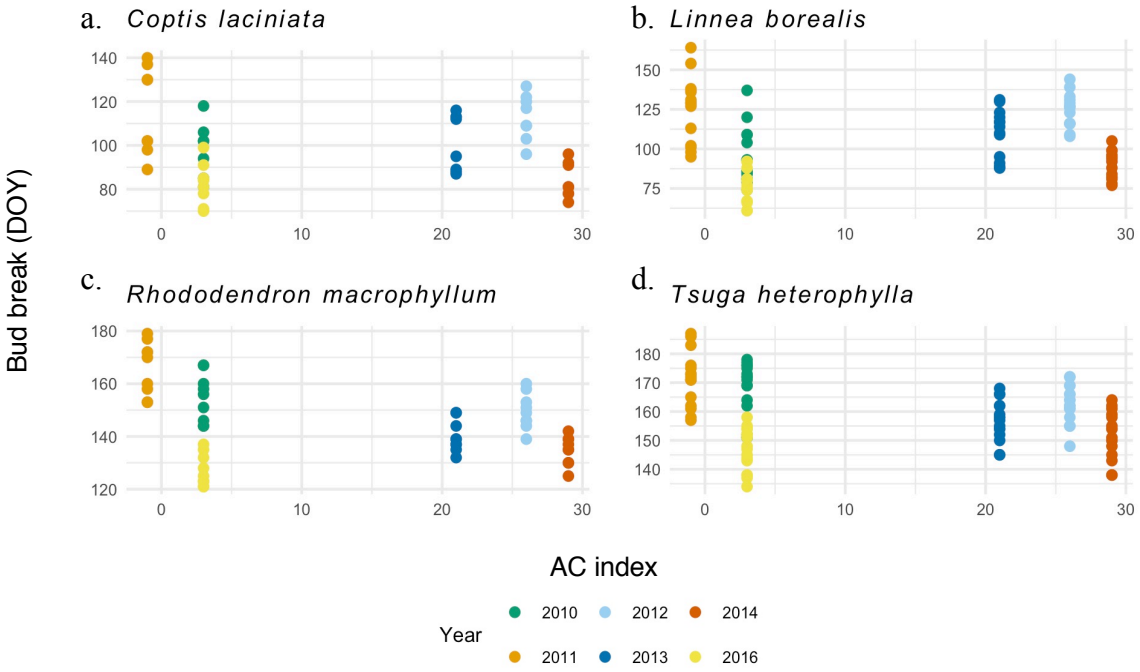

Figure 6: Day of year of bud break relative to AC index. (a) *C. laciniata* (b) *L. borealis* (c) *R. macrophyllum* and (d)*T. hetrophylla.* Colors are year. 2009 and 2015 are not included due to limited sample sizes for a visual comparison of the diversity of bud break.

especially in herbs and shrubs. *Coptis laciniata* and *Linnea borealis* are both herbs, *Rhododenron macrophyllum* is an understory shrub and *Tsuga heterophylla* is a mid-canopy tree.

We explored how elevation affected bud break among individual species across sites and years, by regressing bud break against elevation, and found that in 2015, elevation was a non-significant predictor of bud break in 10 of 14 species (Appendix S1: Table S10). For example, in 2009-2014, and in 2016, elevation predicted between 52% and 86% of the variance in the timing of bud break for *A. circinatum,* but there was no relationship in 2015 (Figure 7a). In contrast, elevation was a significant predictor of bud break for all years for the conifer *Pseudotsuga menziesii* (Douglas fir), and elevation

predicted 94% ($F_{(1,5)}$=87.73, p <2.3e-4) of the variance in bud break during 2015, the highest adjusted R^2 of any year for that species (Figure 7b). This retention of the elevational gradient in the timing of bud break in 2015 was seen in only 4 of 14 species modeled including *Trillium ovatum* (Figure 7c), while 10 of 14 species (including *Vaccinium parvifolium*) saw a complete loss of elevational gradient in bud break (Figure 7d; Appendix S1: Fig S1).

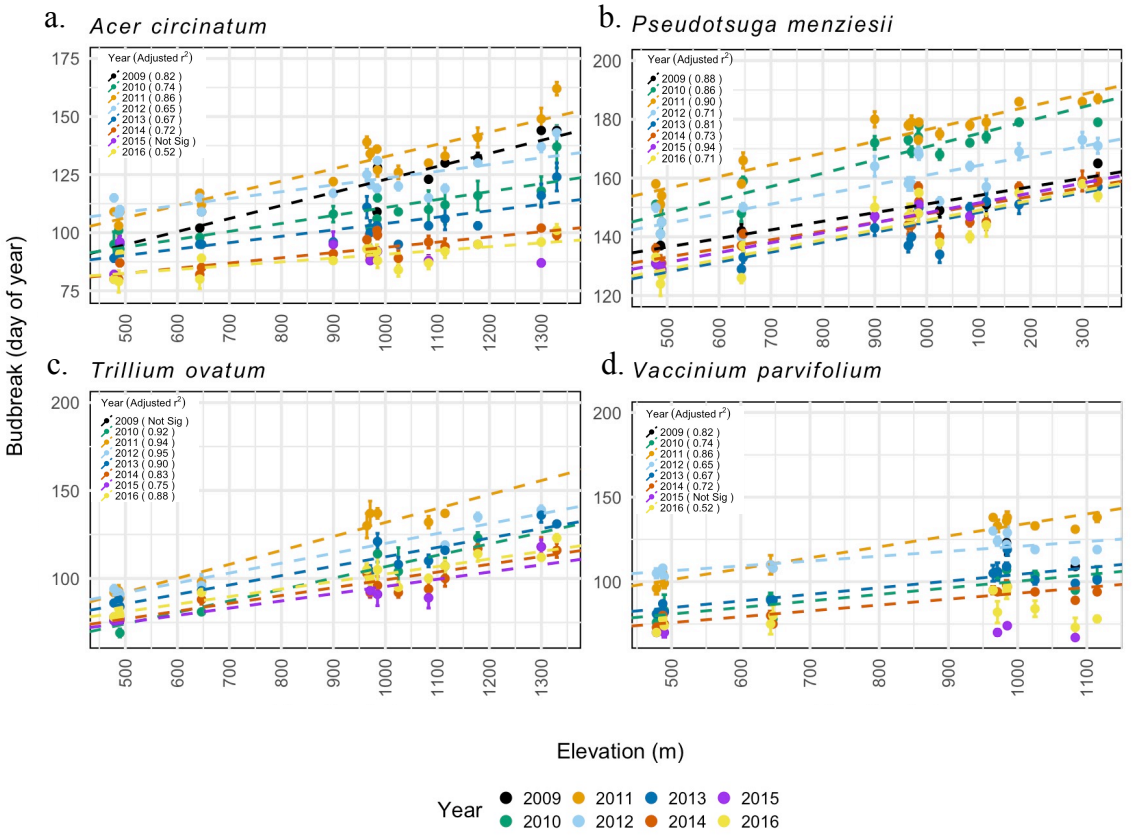

Figure 7: Elevation as a predictor of the timing of bud break. (a) *A. circinatum* (b) *P. menziesii* (c) *T. ovatum* and (d) *V. parvifolium*. Error bars are ± SE, colors are year.

Because 2011 and 2015 represented the extremes in terms of winter climate conditions, we contrast patterns in these two years in many of the figures that follow to illustrate the magnitude of phenological response and variability across the elevational gradient. We saw a median advance of bud break for all species of 37.5 days in 2015 when compared to 2011. The most extreme advancement in bud break occurred at PC09 (984m), where *Viola sempervirens* (violet) broke bud 85 days earlier in 2015 than in 2011 (Appendix S1: Table S7). However, the degree of advancement of bud break was

both species and site specific; e.g., *V. sempervirens* showed as little as 15 days difference between years at a low elevation site (PC01).

Flowering data were limited to those species that regularly flowered over the course of the study, and many of the individuals grow in dense, heavily shaded stands with little opportunity for major reproductive output. Sufficient data (three or more observations at each site, and three or more sites per year) exist for *A. circinatum, Vaccinium parvifolium* (red huckleberry), and *Trillium ovatum* (trillium) to regress the date of peak flower against elevation. Elevation was an inconsistent predictor of variance in the flowering time of *A. circinatum*. We often observed *A. circinatum* flowers aborting/dying prior to reaching peak flowering, which tended to result in low sample sizes and may explain the inconsistent effect of elevation. Elevation explains a large amount of variance in the date of peak flower for *V. parvifolium* during years with typical winter weather, but the elevational gradient is lost in years with low snow like 2015. (Figure 8a). The elevation gradient appears to remain a powerful signal regardless of snowpack for *T. ovatum* (Figure 8b). Both of these species have flowers emerge from rolled leaves, and both species appear to have synced bud break and flowering trends.

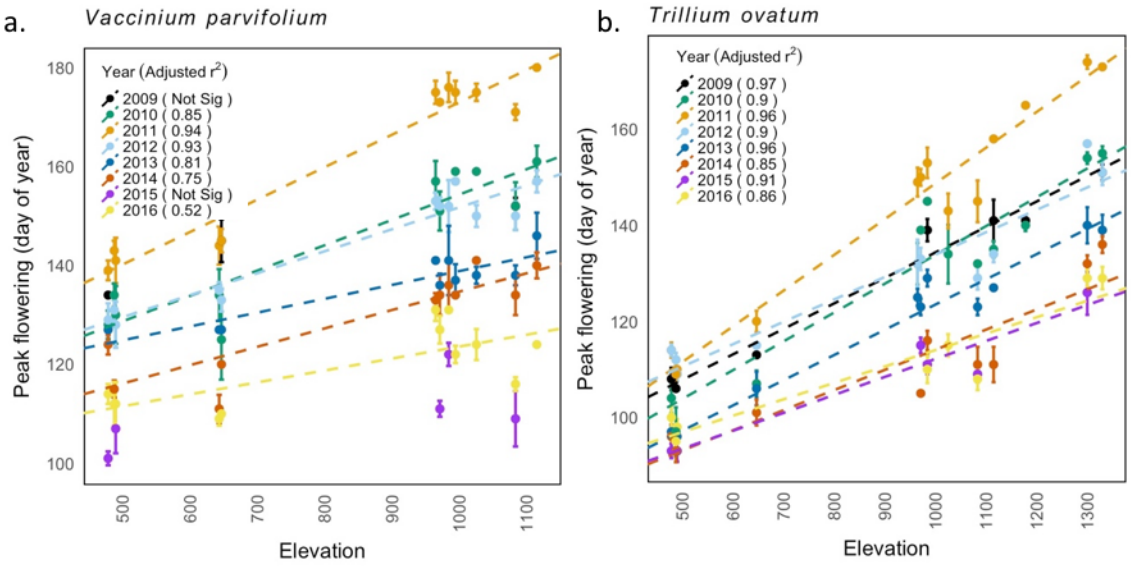

Figure 8: Elevation as a predictor of the timing of peak flowering. (a) V. parvifolium and (b) T. ovatum. Error bars are ± SE.

Discussion

Microclimate is a strong driver of local plant phenology. We found that the combination of unusually warm and dry conditions and the decoupling of areas of low topographic relief from the regional climate patterns can lead to a homogenization of microclimate and spring phenology events in mountainous regions like the Western Cascades. A small number of physical variables explained variation in temperature, especially during winter and spring. Each plant species had a unique response to microclimate variability, and there was considerable variation across and within years. Relatively cool, snowy conditions during winter and early spring led to delayed onset of spring plant phenology (bud break), while relatively warm and dry winter and spring conditions led to an advancement in the onset of spring phenology, especially at upper elevations. In the future, winter and springs with fewer storms, less snowpack, and warm temperatures will likely have advanced bud break across most, if not all species. If areas of low topographic relief are consistently decoupled from regional conditions, and high elevation sites have limited snowpack, there will likely be a homogenization of spring phenology events across the elevation gradient, mainly due to extreme advances at upper elevation sites, especially for herbs and shrubs. A recent study that found similar results where bud break of four European trees advanced ~ 1.9 days per decade from 1960 to 2016 at high elevations (>808 m), and only ~ 0.4 days per decade at low elevations (<522 m) (Vitasse et al. 2018).

Tradeoffs exist for an individual experiencing advanced or delayed bud break (Lockhart 1983, Saxe et al. 2001). Plants that break bud early are subject to a lower solar angle and fewer overall day light hours. This means that primary productivity is limited, and the plant is at risk for frost damage and snow burial, especially at higher elevations (Inouye 2008). We often observed individuals with frost damage on new leaves during years of advanced bud break. If frost damage does not occur, a plant that breaks bud early has a longer growing season, which may result in increased fitness due to greater resource storage, or the plant may be more susceptible to early season drought due to the relatively warm conditions that initiated advanced bud break. In 2015, the warm and dry winter and spring and extraordinarily low snow pack (Sproles et al. 2017) led to early and prolonged drought conditions, reflected in some of the lowest summer flows on record in

Lookout Creek (Johnson and Rothacher 2016). Later bud break and flowering may also result in fewer incidences of fruit set due to less pollination, or less resource allocation towards reserve storage for the winter dormancy period and the following growing season (Rathcke and Lacey 1985, Chapin III et al. 1990, Kreyling 2010).

While our study focused on the herbs, shrubs and trees of the Western Cascades, the effect of advanced phenology is not limited to a single trophic level, and the negative effects of trophic asynchronies have been documented around the world (Parmesan 2006). Insects that depend on new fragile leaves for easy meals may emerge after peak leaf expansion, or after frost damages newly emerged leaves, and find themselves with limited food sources (Visser and Both 2005). Birds dependent on such insects may have less food for themselves and their young. Pollinators may emerge and become active after peak flowering, resulting in less fruit production for the plant, and less food for the pollinator. This in turn could lead to less food for birds and other animals dependent on berry producing species. Areas of topographic heterogeneity typically display a strong gradient in spring plant phenology (Hwang et al. 2011), which may mitigate the effects of regional warming and reduce for mobile organisms like birds or mammals (Gaudry et al. 2015, Frey et al. 2016a). However, in years like 2015, the timing of spring plant phenology became much less varied across microclimates, and it is possible that such loss of variation could lead to more widespread consequences and trophic asynchronies than a relatively cool (late) year in which early season microclimate and phenological diversity are maintained (e.g., 2011). A diverse spread of bud break and flowering events means a longer window of food availability for species able to move from sites with early spring phenology, to sites that begin the growing season later in the year. Losing the diversity across microclimates creates potential for fewer resources for migrants and other mobile species dependent on a varied patchwork of spring flowering and growing seasons.

Since 1979, the northern hemisphere has warmed by 0.33° C per decade (IPCC 2007), and annual average temperatures in the Pacific Northwest are projected to increase by an additional 1.8° C by the 2040s and 3.0° C by the 2080's (Mote and Salathe Jr 2010). This will likely result in more winter precipitation falling as rain and less as snow (Sproles et al. 2013, 2017), and an increase in the range of the transient snow zone, in which snowpack varies throughout the season due to repeated melting and

accumulation) (Mote 2006). Since the 1950s, 92% of snow courses in the western United States have shown negative trends in snowpack (Mote et al. 2018). Lute et al. (2015) predict a reduction of up to 60% of the April 1st snow water equivalent in the Western Cascades, and Sproles et al. (2017) suggest that patterns of snowpack seen in 2014 and 2015 are likely to become more common as warming trends continue. Some models suggest that storms may become less frequent and more severe, resulting in longer windows of clear anticyclonic weather between storms (Pepin et al. 2011). Years with long periods of clear winter weather (e.g., 2015) can lead to persistent temperature inversions in mountainous areas like the Andrews, and valleys and drainages affected by these inversions will have temperatures consistently around freezing (Daly et al. 2010, Pepin et al. 2011, Novick et al. 2016). In contrast, during the same cold air pooling events, upper elevations and ridgelines will be above the inversion and be exposed to consistently clear, sunny weather (Pepin et al. 2011). The combination of less precipitation as snow and more persistent temperature inversions will likely result in a loss of diversity in the timing of spring phenology similar to the pattern we see when comparing the distribution of phenological events in 2015 and 2011. Our data suggest that in the Western Cascades (as opposed to the higher elevation High Cascades, which may not experience a significant decrease in snow pack (Mote 2006), years with little to no snowpack like 2015, and persistent cold air pools will have much greater effects on the mountain communities situated in upper elevation sites and sites of high topographic relief than those communities situated in drainages and lower elevation valleys, and that understory species are more likely to have significant shifts in phenology than overstory trees. Additionally, because sites with less vegetation biomass are less buffered against temperature extremes than sites with old growth characteristics and high biomass (Frey et al. 2016a), understory communities in upper elevation plantations in the Western Cascades will likely have the greatest shifts in phenology due to changes in regional climate patterns. Long term, high resolution (both spatially, i.e. $<1 km^2$, and temporally, i.e. > 2 years) studies such as this one are needed to capture the effects of a warming climate on forest and mountain communities, and to inform managers of vulnerable areas in need of protection. The snow pack of 2015 has been described as "extraordinarily low" (Sproles et al. 2017), and we were fortunate to capture such an

extreme year; a typical two year study would likely have missed the inter-annual variability we captured across the eight years of phenology surveys. As the effects of climate change become more severe, it will be important to understand how regional patterns affect microclimates, and how that in turn affects community dynamics. Identifying which areas across landscapes more and less susceptible to climate change, and the processes responsible for those patterns, is the first step in managing for future conditions (Lawler 2009, Morelli et al. 2016, Lenoir et al. 2017).

CHAPTER III

BRIDGE

The first half of this thesis explained the nuances of inter-annual variability and showed that changes in regional climate patterns (i.e., AC index) have a strong effect on the distribution of microclimate and spring phenology events across the Andrews. I wished to further explore the connection between microclimate and spring phenology and chose four species from the original 18 to develop models with the capacity to predict bud break. I had two goals with this second chapter: 1) to create models that could accurately predict observed bud break using only microclimate variables (i.e., no physical drivers like elevation); and 2) to upscale those models to the landscape level to remotely predict bud break across a wide region.

CHAPTER IV

MODELING BUD BREAK AND MICROCLIMATE

Acknowledgements

This chapter contains co-authored material written by Sarah Ward, Mark Schulze, Bitty Roy.

Introduction

The timing of seasonal plant activity (phenology) is often used as an indicator of a community's response to changes in climate, and in particular, the timing of bud break in plants is a simple and common metric of the onset of spring (Walther et al. 2002). Many studies have found a relationship between rising global temperatures and an advancement in the timing of spring bud break (Parmesan and Yohe 2003, Visser and Both 2005, Parmesan 2006, Menzel et al. 2006, Thackeray et al. 2016), however modeling the effect of climate change on communities across a landscape can be difficult due to the species-specific climatic requirements needed to initiate bud break (Kramer 1994, Chuine et al. 1998, 2000, Cleland et al. 2007). Inter-annual climate variability is a constant for nearly every terrestrial plant in the temperate region, and plants have adapted numerous strategies to avoid breaking bud too early or too late (Kreyling 2010). It is well established that bud break for most species is sensitive to temperature forcing (typically measured as the sum hours above a set temperature threshold, typically 5º C, starting in early winter) (Perry 1971, Polgar and Primack 2011). Many temperate species are also known to require a set amount of chilling units (often defined as degree hours between 0 and 5º C), in addition to accumulating forcing units (degree hours above a set threshold, typically 5º C) that will initiate for the onset of bud break (Hänninen 1995, Bailey and Harrington 2006). This strategy requires a certain period of cold weather before warm weather has an effect on the plant, which prevents the onset of bud break during mid-winter warm spells and mitigates the risk of frost damage to leaves (Heide 2003). However, while recent advances in phenology research have improved our understanding of species-specific bud break requirements (Chiune 2000), the exact physiological requirements of the majority of plants are still unknown (Fitter et al. 1995). Additionally,

even well studied species like *Pseudotsuga menziesii* (Douglas fir) could have local adaptations that lead to physiological differences from what is established in the literature (Bennie et al. 2010).

Advances in remote sensing and modeling techniques have led to an increase in predictions of future phenological shifts due to climate change (Chuine et al. 2000, Reed et al. 2003, Cleland et al. 2007, Buitenwerf et al. 2015). However, the climate a plant experiences is generally at a scale of less than 100m (microclimate), and is strongly affected by local topography and other physical features (Potter et al. 2013, Frenne et al. 2013, Morelli et al. 2016, Frey et al. 2016a). These microclimates can be divergent, or even decoupled from regional weather patterns (especially in winter and early spring) and can make it difficult to predict localized patterns of bud break using low resolution (i.e. >1km) spatial and climate data (Daly et al. 2010, Pepin et al. 2011, Novick et al. 2016, Lenoir et al. 2017).

We were interested in whether we could use microclimate variables to develop species-specific models of bud break for four species native to the Western Cascades using nine years of phenological observations from sixteen sites. Douglas fir, *Acer circinatum* (vine maple), *Vaccinium parvifolium* (red huckleberry) and *Trillium ovatum* (Pacific trillium), are all common native species found in the Western Cascades. Douglas fir is an over story tree that is the dominant species in much of the region (Spies et al. 1990). Vine maple and red huckleberry are both common shrubs that are typical in the understory of both old growth and second growth forests (Brown 1969, Gholz et al. 1976, Agee and Kertis 1987, Kerns et al. 2004), and Pacific trillium is a common herb found across a variety of elevations in the Western Cascades (Brockway et al. 1983). We hypothesized that species-specific models developed at the local scale could be applied to predict bud break across the landscape (Chuine et al. 2000). We hoped to develop models could be used to investigate the local effects of potential shifts in regional climates, such as reduced snow pack, increased temperatures and fewer days of precipitation and cloud cover (Mote 2006, Mote and Salathe Jr 2010, Sproles et al. 2013, Lute et al. 2015).

Areas of heterogeneous topography are known to have a diversity of microclimates (Pepin et al. 2011), which result in a diversity in the timing of

phenological events (Vitasse et al. 2018). These microclimates allow for a longer period of resource availability for organisms that can move with the phenology gradient (Frey et al. 2016a). Additionally, numerous studies have suggested that the microclimate diversity within mountainous areas can buffer against the effects of climate change and that during the glacial and interglacial periods, these buffered areas acted as micro-refugia for biodiversity (Peterson et al. 1997, Dobrowski 2011, Lenoir et al. 2017). While it is uncertain that such buffers will remain stable enough to act as micro-refugia in the future, evidence is mounting that certain microclimatic features maintain cooler conditions despite current patterns of regional warming (Pepin et al. 2011, Frenne et al. 2013, Frey et al. 2016b, Morelli et al. 2016, Frey et al. 2016a). Frey et al. (2016b) found that while high elevation sites in the Western Cascades are typically cooler, and accumulate fewer growing degree days between January and March, vegetation and topography were the dominant factors driving growing degree day accumulation during that part of the year They also found that old growth stands in the Cascade region reduced both the maximum temperature of the warmest month and the average maximum monthly temperature from April to June when compared to closed-canopied plantations (40-60 years old). Given that the phenology of many plant species responds to late winter and early spring temperature forcing (Lavender 1991), this microclimatic buffering of temperature (driven by topography and vegetation) has the potential to mitigate the advancement of phenological events due to regional warming. Models that are developed at the local and landscape scale (rather than downscaling regional models) will be more accurate when identifying microclimates that may be less susceptible to future shifts in regional climate patterns.

Methods

Study area

The H.J. Andrews Experimental Forest is a 6400-hectare (15,800 acre) forest located on the west side of the Cascade Mountains in central Oregon. The area is representative of the Cascade Range, with steep mountainous terrain, exposed ridges and sheltered valleys, and a high degree of topographic heterogeneity with elevations ranging

from 410 to 1630 m. Vegetation is primarily a combination of 150-500 year old mixed conifer forests, and 40-60 year old *Pseudotsuga menziesii* (Douglas fir*)* plantations.

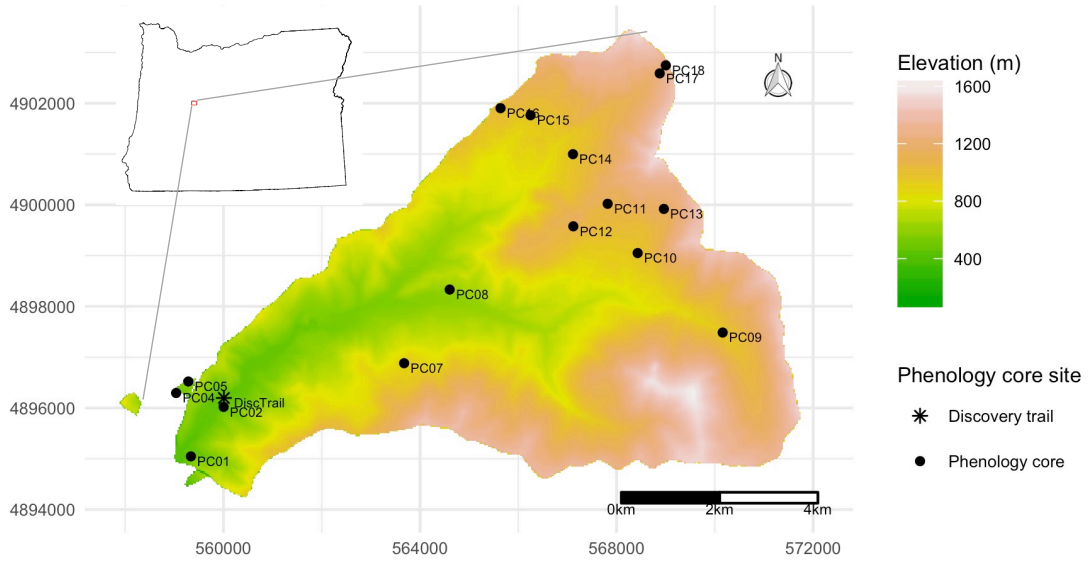

Figure 1: A digital elevation map (dem) of the H.J. Andrews Experimental Forest. Circles triangles are the 16 core phenology sites and the asterix is the location of the Discovery trail. Phenology core sites are labeld with PC and the site number. Color represents elevation, with greens as low elevation sites and light browns as upper elevation sites. Yellows are intermediate elevations

Study design

For the initial phenology study, sixteen sites (core phenology sites) were selected across a variety of elevations and aspects, with sites ranging from 460 to 1339 meters (Appendix S2: Table S1). An additional site (discovery trail) was later added as part of an educational trail, and we used this site, along with 2017 data from the core phenology sites, to validate the bud break models we discuss below (Figure 1). Eighteen species of native herbs, shrubs and trees were permanently marked as target species, and individuals were typically located within 25 m of a center post (occasionally one or two were located up to 35m away to have 5 representatives of each species within a plot). This paper focuses only on four of those species: *Acer circinatum* (Vine maple)*, Pseudotsuga menziesii* (Douglas fir)*, Trillium ovatum* (Trillium) and *Vaccinium parvifolium* (Red huckleberry). We chose these four species because they are common representatives of three functional groups (trees, herbs and shrubs) at the Andrews, and we had a large number of observations of bud break for each species across the study area. Additionally, vine maple and other deciduous shrubs have been shown to support higher levels of

animal and insect diversity and are key factors in within year avian occupancy at the Andrews (Hagar 2007, Ellis and Betts 2011, Frey et al. 2016a).

Understory air temperature was the primary microclimate variable recorded. To capture the temperature of each site, HOBO (Onset Corporation, Hobo U22-001; accuracy 0.2°C) temperature sensors were placed 1.5 meters above the ground facing south in the center of each plot, and temperature data were collected every fifteen minutes. To reduce temperature spikes due to solar radiation, the sensors were placed in the shade, beneath a PVC shield (20.32cm long piece of 7.62 cm schedule 40 pipe split in half lengthwise). Temperature data were assessed for accuracy by comparing phenology data to nearby permanent monitoring sites (Daly and McKee 2016a, 2016b) with long term temperature records. Erroneous data was replaced with data regressed from permanent monitoring sites (Appendix 1, Table S2). Observations of snow depth were made during each visit, however, depth was estimated so only presence or absence data can be used reliably.

Surveys

We developed a species-specific scoring system for vegetative and reproductive phenophases (Schulze 2017). During each spring, sites were typically visited once per week, and each marked individual was scored for vegetative and reproductive growth. In the early years of the study (2009 and 2010), visitations were less consistent, due to concurrent study plot set up and early season site access limitations. From 2011-2017, sites were typically visited once every 7 days. Observations began each year in late winter with the start date varying depending on observed winter weather, snow pack and plant condition across the elevation gradient, with the goal of initiating observations at each site prior to the onset of key phenophases (e.g., bud swell) of focal plant species. In 2015, only a subset of seven sites were visited due to budget and time limitations. To reduce bias (surveys did not always occur on the same day of year each year), all observation dates were standardized to the midpoint of each week, and weeks were defined as day of year weeks (i.e. week three in January begins on 1/15 each year). Occasionally, individuals would exhibit significant development over the course of a week, resulting in missed scores for particular phenophases. For example, a plant may be observed at bud swell one week, and have emerging leaves the subsequent week, with

bud break occurring sometime in the interim. In such cases, we estimated these missed scores by splitting the difference between each observation (e.g., if bud swell was observed on day of year 30 and emerging leaves were observed on day of year 37, we interpolated that bud break occurred on day of year 33). No attempt was made to estimate the timing of phenophases that occurred prior to the first visit of each year, or after the last summer visit.

Modeling bud break:

Final models of bud break were validated using data from the core phenology sites collected in 2017 (not included in the initial model development) and against three years of observations from the discovery trail. These data represent external conditions independent of the original data (internal conditions) used to develop the models. The discovery trail data did not include observations of bud break for Douglas fir, and was not included in the validation of that model. To develop the initial models, we used temperature data (Johnson and Hadley 2017) at each site to calculate forcing, chilling, and frost variables. The two frost variables included were the last day of year when the mean daily temperature was below zero, and the number of days between November 1 and the end of June where the mean daily temperature was below zero. Forcing and chilling units were calculated using models from Harrington et al. (2010), and the chilling variable we included was the day of year at which chilling units reached 1200 (Bailey and Harrington 2006). We calculated two forcing variables, one where forcing units were accumulated beginning on November 1 (in concert with chilling variables) and one where the forcing did not begin to accumulate until the chilling units were greater than or equal to 1200. While the forcing model was developed for Douglas fir trees, we found little literature on appropriate units for the other species, and after initial testing with other established forcing units (namely growing degree days above 5 degrees C and growing degree days above 10 degrees C from January 1), we found both versions of the Harrington forcing model (i.e. simultaneous accumulation and accumulation after a set threshold) to have the most predictive power. We included forcing accumulated on the first of April, May and June from November 1st and after 1200 hours of chilling were accumulated. We also calculated mean April temperature, as an indicator of the relative warmth of the spring regardless of the earlier winter conditions. We used presence or

absence of snow observed during the closet visit to the first of April and the first of May as snow metrics. All data was examined prior to modeling and transformed to reduce skew where necessary.

For vine maple, red huckleberry and trillium, we tested two initial sets of variables (Table 1). We chose to test one model that included simultaneous forcing and chilling, and another that included forcing after chilling, we did not know whether these plants respond to forcing accumulated at the same time as chilling or forcing that does not begin accumulating until after a set chilling unit was reached. For Douglas fir, we included both types of forcing variables in one model, as we only included forcing on June1, and assumed the model selection would select one of the two forcing metrics.

Table 1: Variables included initial bud break models.

Vine maple, Red huckleberry and Trillium : Forcing^{+}	Vine maple, Red huckleberry and Trillium : Chilling^{+}	Douglas fir
Days below 0	Days below 0	Days below 0
Last day of year below 0	Last day of year below 0	Last day of year below 0
April 1 snow (0 or 1)	April 1 snow (0 or 1)	April 1 snow (0 or 1)
May 1 snow (0 or 1)	May 1 snow (0 or 1)	Mean April temperature
Mean April temperature	Mean April temperature	June forcing (from Nov. 1)
Day of year when chilling units = 1200	May 1 forcing.chilling x April 1 snow	June forcing (after 1200 chilling units)
May 1 forcing^{+} x April 1 snow	OR	Day of year when chilling units = 1200
OR	April 1 forcing.chilling x April 1 snow	
April 1 forcing^{+} x April 1 snow		

+For vine maple, red huckleberry and trillium four versions of the model were tested: Forcing from November 1 to April 1; forcing after chilling to April 1; forcing from November 1 to May 1; forcing after chilling to May 1. This was due to high correlation between the two months.

All species models were initially reduced using best subsets (rpackage leaps, Appendix S3) which gives two potential models for each number of available variables (i.e., if there are 3 variables, leaps outputs two models with one variable, two with two variables etc.) and a Mallows CP score and an adjusted R^2 value for each model. We always tested the model with the highest adjusted R^2 and the lowest Cp score; however if that model had significant multicollinearity (variance inflation factors identified via r base function vif(), Appendix S3), we removed the variable with the highest vif score and tested the reduced model. See Appendix S2: Table S3 for all tested models. We selected

the final model based on the prediction accuracy of observed validation data (Appendix S2: Table S4). Accuracy was determined via the coefficient of determination (R^2) from a linear regression of observed versus predicted dates of bud break. If two models were nearly identical in their predictive power, we favored models that most accurately predicted the discovery trail data, as it was completely independent of the original model development. Assumptions of linear models were checked for each model.

Modeling microclimate

To upscale the models at the landscape level, we needed to predict the temperature variables included in each species model. We used available spatial data (Valentine and Lienkaemper 2005, Valentine and DeSilva 2014, Spies 2015, 2016), to predict all of the microclimate included in each species model and created 30m resolution rasters with each temperature variable across the Andrews for 2009-2016. To model snow, we used snow depth data from an existing network of snow stakes that have been visited approximately once every three weeks during the winter from 1998 to 2014 (Schulze and Levno 2017) and created a binary presence absence variable for the first of each month between December and June. Because the sites were not always visited precisely on the first of each month, we considered any survey that occurred within four days on either side of the first to be representative of the snow depth on the first of the month. We used stepwise logistic regression to select the snow model (rpackage MASS, Appendix S3) with AIC as the selection criteria, and initially included the depth of snow on the date of interest at two permanent meteorological stations (CENMET and UPLMET, 1028 m and 1284 m respectively), aspect, biomass and elevation, and mean monthly air temperature at one low and high elevation meteorological stations (PRIMET, 436 m; UPLMET 1284m) (Daly and McKee 2016b). For all variables except snow, we used multiple linear regression and stepwise model selection. The initial models included observed temperature metrics from the phenology sites as predicted by relative topographic position (i.e. ridge or valley), biomass, slope and elevation, mean temperature at PRIMET and two anticyclonic-cyclonic indices (AC index) (Table S5). The AC index is a metric used by Daly et al (2010) (data courtesy of Chris Daly) and can indicate the frequency anticyclonic versus cyclonic weather systems over a given period of interest and thereby the frequency of temperature inversions. Anticyclonic weather

patterns result in cold air pooling and decoupling of valleys and depressions from regional weather, particularly in winter and early spring. With cyclonic weather systems, temperatures across the Andrews Forest elevation gradient typically conform to expectations based on moist adiabatic lapse rates, whereas in periods with anticyclonic systems, valleys maintain temperatures near freezing, and ridges and slopes are exposed to clear weather and higher daily temperatures due to increased irradiation (Daly et al. 2010, Pepin et al. 2011). Hence, a relatively warm winter with no shift in the AC index would be expected to preserve a strong elevational gradient in average air temperature, whereas a shift in the AC index could result in homogenization of mean or cumulative temperature metrics such as forcing units. We used the AC index from November to May (for June forcing. chilling) and from November to March (for April forcing/April forcing. chilling) as an annual constant that represents the inter-annual variability of regional climate and is an indicator of local climatic decoupling due to cold air pooling. We also included two mean temperature variables (mean April temperature and mean temperature between November 1 and May 31) from the low elevation meteorological station (PRIMET, 436 m), and a snow depth variable for the first of the month for April and May from a mid and a high elevation meteorological station (CENMET,1025 m; UPLMET 1284 m, MS001) as indicators of the annual conditions (Daly and McKee 2016b). We tested the predicted climate models against four years (2011-2014) of data from 180 sites across the Andrews (Johnson and Hadley 2017). While this validation data set is more spatially robust, we chose to model the phenology temperature data as it is more temporally robust and includes data from all of the phenology survey years. We do not have AC index data for 2017, and so we tested the upscaled landscape models against the observed 2009-2016 phenology core data and discovery trail data.

Results

Bud break models

We succesfully developed bud break models for all four species with a range of preditive success, both for internal (original 2009 to 2016 data) and external (2017 and Discovery trail validation data) conditions (Figure 2, Table 2). All four models were quite accurate when predicting the orignal phenology data and the validation data (Table

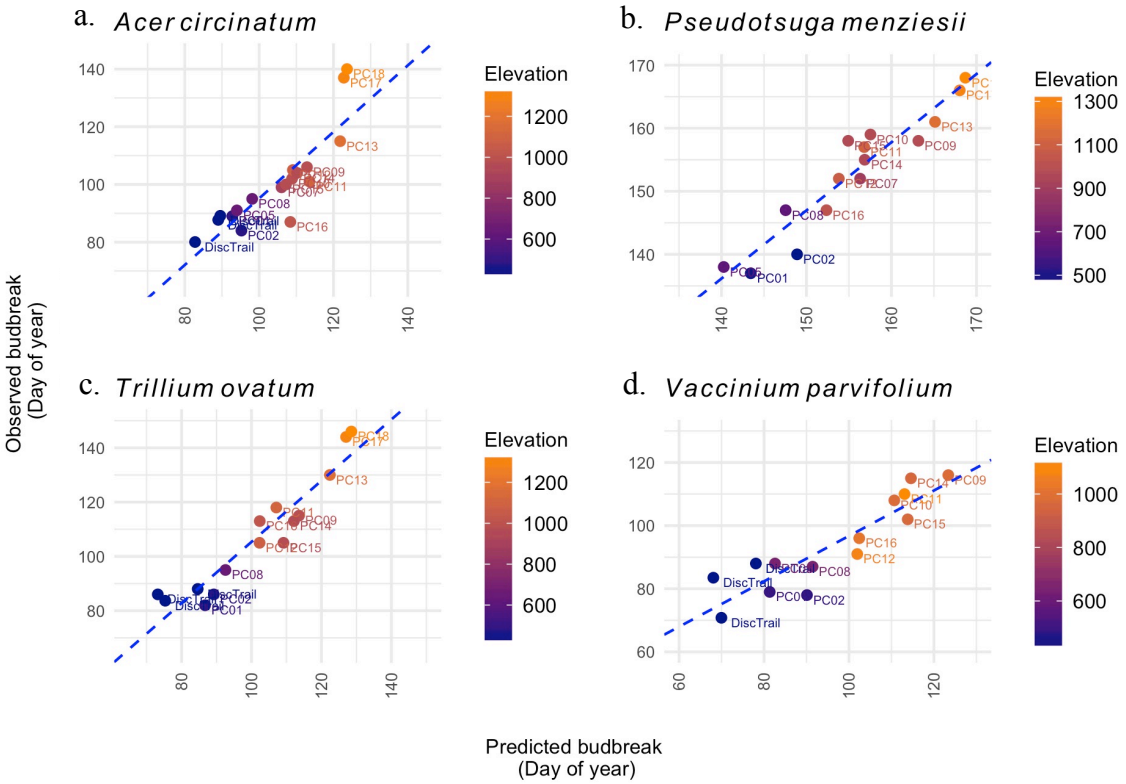

Figure 2: Observed bud break for 2017 and discovery trail data versus bud break predicted by species models. (a) *Acer circinatum*; (b) *Pseudotsuga menziesii*; (c) *Trillium ovatum*; (d)*Vaccinium parvifolium*. Colors are elevation, with oranges indicating high elevation sites, and blues indicating low elevation sites, with reds as intermediate values. Sites are labeled as PC and the site number for phenology core sites or Disc. Trail for the discovery trail.

3). The vine maple model included mean April temperature, total days below and the first day of year where chilling uniits were greater than 1200. The model explained 73% of the variance in the 2009-2016 data and 74% of the variance in the validation data. The model for Douglas fir was surprisingly simple and only included June 1 forcing after chilling as a predictive variable. The model explained 83% of the variance in the original dataset 90% of the variance in the validation data. The trillium model was also highly successful and included observed presence or absence of snow on April 1, total days below 0 and mean April temperature; the model explained 85% of the variance in the original dataset and 90% of the variance in the validation data. Finally, the model for red huckleberry explained 82% of the variance in the original data, and 81% of the variance in the validation data. This included mean April temperature, the last day of year below freezing and April 1 forcing after chilling.

Table 2: Varibles included in each bud break model

Species	Model variables and coefficients[+]	Cp Score	R^2	F-stat	P-value
Acer circiantum	Budbreak (DOY) = e^(4.67 – 0.04 x MAT + 0.04 x (√DB0) – 0.03 x (√DOY@1200))	2.79	0.73	$94.72_{(3,107)}$	***
Pseudotsuga menziesii	Budbreak (DOY) = 179.68 – 0.09 x JFC	18.55[+++]	0.83	$510_{(1,105)}$	***
Trillium ovatum[++]	Budbreak (DOY) = (10.05 + 0.20 x A.snow + 0.48 x (√DB0) – 0.25 x (MAT))^2	5.42	0.85	$125.1_{(3,64)}$	***
Vaccinium parvifolium[++]	Budbreak (DOY) = (9.86+ 0.20 x LD0 - 0.30 x MAT – 0.52 x ln(AFC))^2	0.09	0.82	$110.6_{(3,73)}$	***

+ AF = April forcing (from Nov.1); AFC = April forcing after chilling; A.snow = April 1 snow; DB0 = Number of days below 0 between November 1 and June 1; DOY@1200 = First day of year where 1200 chilling hours are accumulated; JFC = June forcing after chilling; LD0 = Last day of year below 0; MAT = Mean April temperature

++ Predictor variables scaled (mean centered) using r function scale() to reduce collinearity; scaling occurred after any transformation of data.

+++ Despite a high CP score, all other potential models had highly correlated variables and R^2 values that differed only by around 0.01.

Table 3: Model statistics for the 2017 and discovery trail validation data

Species	R_2	$F\text{-stat}_{(df)}$	p-value
Acer circinatum	0.74	$45.91_{(1,16)}$	***
Pseudotsuga menziesii	0.90	$112.1_{(1,13)}$	***
Trillium ovatum	0.90	$110.5_{(1,13)}$	***
Vaccinium parvifolium	0.81	$50.78_{(1,12)}$	***

Microclimate models

We were able to successfully model all of the predictive climate variables across the Andrews watershed (Appendix S2: Table S6). The microclimate models explained between 63% and 81% of the variance in the validation data for all variables except for April forcing after chilling (Table 4). The model for April forcing after chilling

explained 35% of the variance in the validation data. For snow, we used a logistic regression, and compared observed snow at snow stake sites between 2014 and 2015 and found that sites with observed presence of snow had a mean probability of 0.64, and sites with no snow had a mean probability of 0.27 (Table S8). We applied the bud break models to the new microclimate rasters and predicted bud break across the entire Andrews watershed, and tested the validity against the 2009 to 2016 observed phenology data (Table S9, Figure S1).

Table 4: Model statistics from validation of microclimate variables.

Microclimate variable	F-stat$_{(df)}$	R^2	p-value
April chilling after forcing	$282.6_{(1,533)}$	0.35	***
DOY chilling above 1200	$889.4_{(1,533)}$	0.63	***
Mean April temperature	$2325_{(1,533)}$	0.81	***
Days below 0	$891.3_{(1,533)}$	0.63	***
Last day of year below 0	$1023_{(1,533)}$	0.66	***
June forcing after chilling	$1162_{(1,533)}$	0.69	***

To explore the possibility of identifying microclimates less susceptible to warming trends, we compared the two years with the highest and lowest values of each predicted microclimate variable. June forcing after chilling, the day of year where 1200 chilling units are accumulated, number of days below 0 and April forcing after chilling all had distinct patterns of microclimate distribution, with some areas experiencing a much greater range of values than others (Figure 3). High elevation sites saw much greater ranges in both the day of year where chilling reached 1200 and the last day of year where the temperature dropped below 0. Low elevation sites tended to see greater ranges in forcing metrics, although the April 1 forcing appears to be buffered near the stream channels, even when nearby areas show extreme ranges in April 1 forcing units.

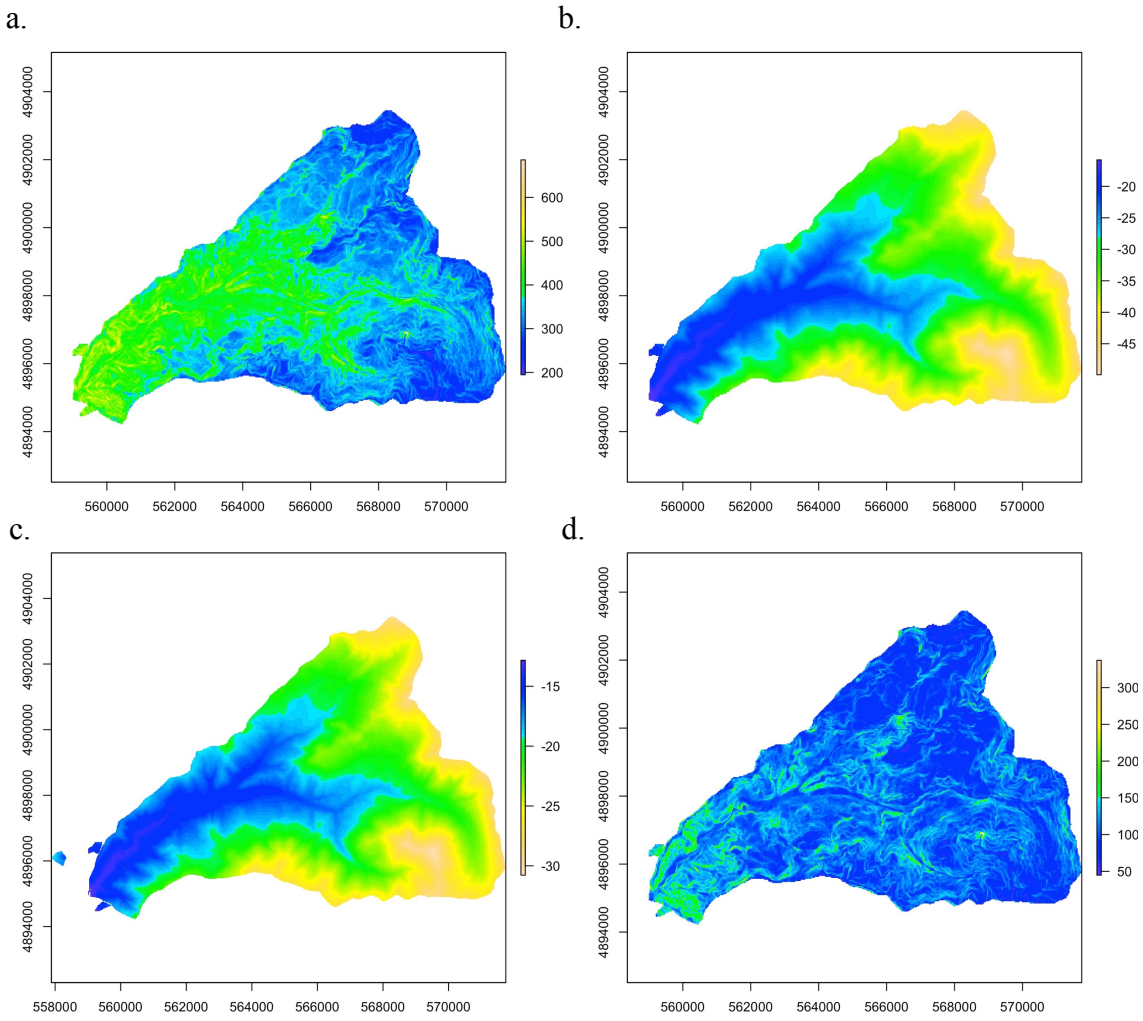

Figure 3: Range in microclimate variables across the Andrews between the warmest (2015) and coolest (2011) years in the phenology record. (a) June forcing after chilling. (b) Number of days below 0. (c) First day of year above 1200 chilling units. (d) April forcing after chilling. All colors represent the range between 2011 and 2015 values (2015 was the warmest year in the phenology record while 2011 was the coolest). Blues represent regions with the least range in the given variable, while yellows are the areas with the greatest range between the two years. Greens are intermediate.

Discussion

We were able to create species-specific models of bud break that were robust for predicting both internal and external (validation) data. The Douglas fir model was highly accurate across all elevations, with a median difference of 2.26 days, and a maximum difference between observed and predicted data of 8.9 days (Table S11). Interestingly, the model for Douglas fir included the forcing variable that accumulated

after 1200 chilling units rather than a forcing variable that accumulates simultaneously with chilling (parallel model). This is counter to Harrington et al. (2010), whose models of forcing and chilling units we used. They modeled Douglas fir bud break possibility lines using chilling and forcing units that accumulated simultaneously. However, other studies have supported temperate trees requiring a certain number of chilling units prior to forcing accumulation (sequential model) (Landsberg 1974, Hänninen 1995, Bailey and Harrington 2006). Because the Harrington *et al.* models were developed using seed sources that had a maximum elevation of 880m, it is possible that the individuals from our study have a more rigid chilling requirement as individuals that break bud too early at higher elevations will more likely be subject to frost damage. Red huckleberry also included forcing after chilling, which was surprising. We tend to (anecdotally) observe huckleberry rapidly breaking bud as soon as daily temperatures begin to warm up. It's possible that the day of year when chilling is near 1200 units is also closely timed with snow melt, and the variable is a stand in for the more direct effect of snow. Neither models for vine maple or trillium had any forcing metrics included, and both included mean April temperature and the number of days below 0. Because both species are subject to snow burial and persistent freezing temperatures beneath temperature inversions, it is possible that mean April temperature captures the late season forcing that occurs after snow melts and the number of days below 0 indicate the persistence of cold air pooling events.

The models for trillium and vine maple were both the least accurate when predicting bud break at the two highest elevation sites (PC17 at 1300 m and PC18 at 1330 m) (Table S4). Both of these species are subject to winter snow burial, and it is likely that our snow variable (presence or absence at the site) does not capture the fine scale nuances of snow pack (and snow melt) that affect an individual plant, and thus the bud break models fail to capture as much variance as the other species less affected by snow (i.e. Douglas fir). The vine maple model also predicted a later bud break at PC16. This site is a mid to high elevation site (1025m) that is situated at the top of a south facing ridge that is often much more advanced than other sites at the same elevation. The model predicted bud break 17 days later than the observed value and as there is rarely a late

season snow pack at this site, it is likely that some of the finer nuances of microclimate are not captured in the overall model.

We were able to accurately predict microclimate across the landscape using only a few sites. When comparing the two extreme years, we found that the low elevation stream sites were buffered against extreme variability in freezing events and the rate of chilling accumulation, while high elevation sites were buffered against extreme ranges in June forcing metrics. The range in April forcing after chilling was particularly interesting, as the low elevation stream valleys showed little variability while sites only a few hundred meters up the hillsides showed extreme ranges in April forcing accumulation. Further exploration of historic data may indicate sites that are consistently buffered against extreme climate variability.

Conclusions

Vegetation and topography are the dominant factors driving winter and spring temperature in the Western Cascades, and areas of heterogeneous topography and high biomass (i.e., old growth forests) have the potential to buffer species from regional increases in winter and spring temperature (Pepin et al. 2011, Frenne et al. 2013, Frey et al. 2016b, Morelli et al. 2016, Frey et al. 2016a). However, identifying potential microclimates is difficult due to the highly variable physiologies of individual species. We found that physical variables and temperature metrics from a few local sites can be used to accurately predict microclimate across a landscape, and species-specific models can then be applied to a broad area. Upscaling species-specific bud break models derived from a local scale has the potential both explore the effects of future climate scenarios, and to identify sites that may continue to maintain microclimatic diversity in the future. These sites could benefit or protect those species most susceptible to a homogenization of microclimates and phenologies driven by warming climate trends.

CHAPTER V

CONCLUSION

In summary, we found that during the eight year phenology study, years with a decline in winter snow pack, and an increase in cold air pooling events resulted in a more similar distribution of microclimates across a watershed. This homogenization of microclimates led to a less diverse range of spring phenology events, especially in herbs and shrubs. Microclimate is a significant driver of spring plant phenology, and local temperature metrics can be used to accurately predict phenology across a wide range of microclimates. Snow is likely the most limiting factor in modeling plant phenology, especially for herbs and shrubs, as it is difficult to measure at a high enough resolution. The models we developed tended to predict bud break early than observed at sites with persistent snow pack. Finally, physical variables can be used to accurately predict microclimate across a landscape, using observed data from only a few sites. These up scaled microclimate variables can be used to accurately predict bud break across the landscape and have the potential to help identify local zones that are protected from the predicted changes in regional climate.

APPENDIX A

APPENDIX S1

Table S1: Species list for plants included in phenology study.

Species	Common name	Species code
Abies amabilis	Pacific silver fir	ABAM
Abies procera	Noble fir	ABPR
Acer circinatum	Vine maple	ACCI
Acer macrophyllum	Big leaf maple	ACMA3
Chimaphila umbellata	Princes pine	CHUM
Coptis laciniata	Cut-leaf goldthread	COLA3
Cornus canadensis	Bunchberry	COCA13
Cornus nutalii	Pacific dogwood	CONU4
Linnaea borealis	Twinflower	LIBO3
Pseudotsuga mensiezii	Douglas fir	PSME
Rhododendron macrophyllum	Pacific rhododendron	RHMA
Rubus ursinus	Creeping blackberry	RUUR
Synthyris reniformis	Snow queen	SYRE
Trillium ovatum	Trillium	TROV2
Tsuga hetrophllya	Western hemlock	TSHE
Vaccinium membranaceum	Mountain huckleberry	VAME
Vaccinium parvifolium	Red huckleberry	VAPA
Viola sempervirens	Violet	VISE3

Table S2: Regression equations used to fill in any missing or erroneous temperature data.

Site	Equation	Adjusted R^2	df	F-stat	P-value
PC01	PC01 = RS02 x 0.941 + 0.649	0.989	1,45215	425924	***
PC02	PC02 = CS2met x 0.933 + 1.074	0.986	1,49115	354185	***
PC04	PC04 = RS89 x 0.985 + 0.632	0.994	1,54915	979041	***
PC05	PC05 = RS86 x 0.992 + 0.430	0.994	1,44049	706341	***
PC07	PC07 = RS05 x 0.987 - 0.075	0.996	1,55057	1271158	***
PC08	PC08 = RS10 x 1.000 + 0.115	0.997	1,54568	1571495	***
PC09	PC09 = RS12 x 1.001 + 0.381	0.992	1,53536	647952	***
PC10	PC10 = RS05 x 1.003 - 0.568	0.986	1,54745	376250	***
PC11	PC11 = RS26 x 0.975 - 0.554	0.991	1,47045	495211	***
PC12	PC12 = RS26 x 0.979 + 0.107	0.996	1,54593	1402571	***
PC13	PC13 = RS26 x 0.952 - 1.235	0.971	1,54196	181439	***
PC14	PC14 = RS05 x 1.016 - 0.454	0.989	1,55067	485521	***
PC15	PC15 = HI15 x 0.984 + 0.386	0.985	1,48635	320198	***
PC16	PC16 = RS26 x 0.996 - 0.026	0.986	1,54059	372480	***
PC17	PC17 = RS04 x 0.977 + 0.014	0.992	1,47550	595117	***
PC18	PC18 = RS04 x 1.001 - 0.203	0.984	1,48787	308451	***

Notes

-- Non Significant; * P<0.05; ** P<0.01; ***P<0.001; In the site column, PC represents "phenology core"; In the equation column, all abbeviations following = are representative of reference stands (RS) or other climate stations (HI15 and CS2met); df, degrees of freedom.

Table S3: Variables included in principle component analysis of temperature data.

Temperature PCA Variables	Description:
Winter average	Mean temp between January 1 and March 31
Spring average	Mean temperature between April 1 and June 30
Summer average	Mean temperature between July 1 and September 30
Fall average	Mean temperature between October 1 and December 31
Annual average	Mean temperature between January 1 and December 31
Winter GDD	Accumulated growing degree days above 5° C between December 1 and March 31
Spring GDD	Accumulated growing degree days above 5° C between April 1 and June 30
Minimum: coldest month	Minimum temperature (°C) of the coldest month per year (Nov 1 – Oct 31)
Maximum: warmest month	Maximum temperature (°C) of the warmest month per year (Nov 1 – Oct 31)
Mid winter average	Mean temperature between December 1 and March 31

Table S4: Variable contributions to each principle component in Figures 2a and 2b

Variable	PC1	PC2
Winter average (Jan – Mar)	12.84	0.36
Spring average (Apr – Jun)	12.40	0.00
Summer average (Jul – Sept)	8.39	2.78
Fall average (Oct – Dec)	0.13	89.44
Annual average (Jan – Dec)	15.24	0.03
Winter GDD (Dec – Mar31)	11.99	0.46
Spring GDD (Apr 1- Jun 30)	12.70	0.05
Minimum temp (Jan – Dec)	6.54	1.73
Maximum temp (Jan – Dec)	6.14	4.97
Mid winter average (Dec-Mar31)	13.62	0.17

Table S5: Growing degree days for all sites and all years for the first six months of each year (January 1 to June 30), and for winter (December 1 – March 31).

Plot	Elevation	2009	2010	2011	2012	201	2014	2015	2016
PC01	489.47	635.33 (35.52)	528.07 (104.32)	428.98 (52.35)	548.37 (41.67)	697.21 (74.8)	705.31 (96.82)	939.72 (242.63)	830.28 (123.19)
PC02	478.21	627.46 (29.47)	478.48 (68.18)	399.52 (36.3)	502.08 (23)	649.05 (55.17)	625.31 (69.21)	833.7 (164.8)	745.66 (90.4)
PC04	487.25	666.87 (42.28)	555.44 (113.95)	443.25 (51.98)	571.56 (44.53)	720.77 (82.47)	713.32 (106.5)	950.91 (249.18)	829.44 (120.07)
PC05	643.14	764.49 (115.82)	586.08 (144.05)	472.97 (80.73)	614.53 (87.3)	770.96 (107.09)	794.44 (165.14)	1051.37 (299.24)	887.67 (137.31)
PC07	899.88	474.95 (26.44)	304.89 (37.22)	245.99 (26.06)	357.03 (14.93)	484.7 (21.72)	494.08 (64.38)	748.45 (166.4)	607.17 (55.57)
PC08	646.51	624.44 (46.01)	480.94 (94.98)	381.69 (49.4)	510.61 (39.08)	654.04 (61.66)	667.99 (99.92)	909.35 (228.03)	775.86 (98.68)
PC09	985	389.81 (3.38)	258.79 (19.48)	176.47 (5.35)	286.41 (6.15)	398.86 (6)	416.36 (29.89)	649.12 (113.67)	501.49 (23.95)
PC10	984	446.6 (19.88)	294.39 (44.85)	207.96 (14.89)	330.2 (17.71)	439.42 (17.53)	468.12 (60.46)	711.66 (161.27)	584.08 (52.65)
PC11	1114.83	473.86 (69.35)	287.82 (54.18)	205.4 (26.87)	339.29 (39.58)	442.84 (37.09)	486.77 (110.42)	734.98 (195.11)	574.76 (68.29)
PC12	1083.18	524.94 (87.2)	330.67 (78.65)	245.1 (48.7)	389.3 (66.34)	508.25 (68.73)	540.42 (141.98)	821.81 (247.79)	650.93 (104.68)
PC13	1177.89	402.41 (50.84)	203.68 (22.34)	116.31 (5.02)	233.58 (13.97)	338.42 (4.85)	371.35 (55.98)	619.73 (135.36)	446.32 (19.84)
PC14	964.54	469.42 (23.21)	291.9 (35.14)	210.11 (9.29)	335.93 (12.37)	458.43 (12.13)	486.75 (62.98)	744.67 (158.55)	590.56 (41.28)
PC15	970.83	500.57 (33.44)	317.48 (43.2)	225.63 (12.25)	360.79 (15.95)	483.95 (12.96)	523.3 (75.55)	814.07 (181.33)	634.39 (50.34)
PC16	1025.07	546.23 (84.86)	373.03 (83.01)	266.9 (40.1)	410.94 (53.53)	524.65 (54.23)	523.3 (75.55)	838.41 (242.65)	668.02 (97.45)
PC17	1299.86	386.89 (63.08)	176.65 (12.91)	96.61 (3.96)	225.45 (13.28)	340.02 (39.81)	347.68 (64.39)	601.68 (124.5)	408.91 (14.74)
PC18	1329.72	392.32 (63.5)	191.38 (15.09)	111.75 (8.65)	231.67 (13.16)	342.39 (40.68)	355.88 (60.88)	602 (121.24)	417.97 (29.09)

Notes

Data outside the parentheses is January 1 – June 30 growing degree day accumulation, while data within parentheses is winter growing degree days (December 1 – March 31).

Table S6: A-C index values between December 1- March 31 from 2009 to 2016.

Year	AC index
2009	12
2010	3
2011	-1
2012	26
2013	21
2014	29
2015	44
2016	3

Table S7: Snow data for all sites and years.

Plot	Elevation (m)	Year	Estimated last DOY with patchy snow	Estimated max days of snow (Dec 1 – Mar 31)	DOY with no buried plants observed
PC01	489.47	2009	96	35	NA
PC02	478.21	2009	96	35	NA
PC04	487.25	2009	96	35	NA
PC05	643.14	2009	105	35	NA
PC07	899.88	2009	105	45	NA
PC08	646.51	2009	105	35	NA
PC09	985	2009	120	63	NA
PC10	984	2009	110	50	NA
PC11	1114.83	2009	133	70	NA
PC12	1083.18	2009	132	50	NA
PC13	1177.89	2009	141	82	NA
PC14	964.54	2009	125	70	NA
PC15	970.83	2009	110	60	NA
PC16	1025.07	2009	110	60	NA
PC17	1299.86	2009	145	88	NA
PC18	1329.72	2009	150	92	NA
PC01	489.47	2010	91	7	62
PC02	478.21	2010	91	7	48
PC04	487.25	2010	91	7	55
PC05	643.14	2010	95	10	55
PC07	899.88	2010	105	15	62
PC08	646.51	2010	95	10	48
PC09	985	2010	123	39	125
PC10	984	2010	102	15	48
PC11	1114.83	2010	139	46	132
PC12	1083.18	2010	127	35	48
PC13	1177.89	2010	137	61	132
PC14	964.54	2010	121	47	125

PC15	970.83	2010	121	47	125
PC16	1025.07	2010	121	47	132
PC17	1299.86	2010	149	87	153
PC18	1329.72	2010	149	92	153
PC01	489.47	2011	91	7	75
PC02	478.21	2011	118	7	75
PC04	487.25	2011	91	7	75
PC05	643.14	2011	82	7	82
PC07	899.88	2011	116	45	103
PC08	646.51	2011	105	7	103
PC09	985	2011	137	45	152
PC10	984	2011	128	57	131
PC11	1114.83	2011	150	75	152
PC12	1083.18	2011	132	57	138
PC13	1177.89	2011	158	105	159
PC14	964.54	2011	147	80	145
PC15	970.83	2011	137	90	145
PC16	1025.07	2011	137	90	131
PC17	1299.86	2011	166	110	173
PC18	1329.72	2011	166	110	180
PC01	489.47	2012	87	7	88
PC02	478.21	2012	87	7	88
PC04	487.25	2012	87	7	81
PC05	643.14	2012	99	15	102
PC07	899.88	2012	92	7	109
PC08	646.51	2012	96	35	88
PC09	985	2012	152	55	130
PC10	984	2012	116	50	116
PC11	1114.83	2012	122	55	116
PC12	1083.18	2012	107	7	116
PC13	1177.89	2012	126	65	137
PC14	964.54	2012	126	65	123
PC15	970.83	2012	121	60	123
PC16	1025.07	2012	108	50	116
PC17	1299.86	2012	144	70	144
PC18	1329.72	2012	146	70	165
PC01	489.47	2013	91	7	72
PC02	478.21	2013	91	7	72
PC04	487.25	2013	91	7	72
PC05	643.14	2013	91	7	72
PC07	899.88	2013	104	7	93
PC08	646.51	2013	91	7	79
PC09	985	2013	120	45	121

PC10	984	2013	112	7	107
PC11	1114.83	2013	112	7	114
PC12	1083.18	2013	110	7	114
PC13	1177.89	2013	112	45	121
PC14	964.54	2013	112	45	114
PC15	970.83	2013	112	45	114
PC16	1025.07	2013	112	45	114
PC17	1299.86	2013	130	65	128
PC18	1329.72	2013	130	65	135
PC01	489.47	2014	91	7	57
PC02	478.21	2014	91	7	57
PC04	487.25	2014	91	7	57
PC05	643.14	2014	91	7	57
PC07	899.88	2014	91	7	71
PC08	646.51	2014	91	7	71
PC09	985	2014	91	7	120
PC10	984	2014	119	14	99
PC11	1114.83	2014	119	28	120
PC12	1083.18	2014	96	14	120
PC13	1177.89	2014	126	35	120
PC14	964.54	2014	119	14	99
PC15	970.83	2014	118	14	120
PC16	1025.07	2014	118	14	99
PC17	1299.86	2014	119	28	127
PC18	1329.72	2014	126	42	127
PC01	489.47	2015	1	0	1
PC02	478.21	2015	1	0	1
PC07	899.88	2015	1	0	1
PC09	985	2015	1	7	47
PC12	1083.18	2015	102	7	47
PC15	970.83	2015	1	7	1
PC17	1299.86	2015	117	14	102
PC01	489.47	2016	40	14	47
PC02	478.21	2016	75	21	83
PC04	487.25	2016	75	21	83
PC05	643.14	2016	40	14	47
PC07	899.88	2016	83	56	89
PC08	646.51	2016	75	21	83
PC09	985	2016	92	96	96
PC10	984	2016	83	96	89
PC11	1114.83	2016	91	63	96
PC12	1083.18	2016	80	56	90
PC13	1177.89	2016	91	103	96

PC14	964.54	2016	89	56	96
PC15	970.83	2016	89	56	96
PC16	1025.07	2016	89	56	93
PC17	1299.86	2016	97	134	124
PC18	1329.72	2016	97	134	124

Notes

In 2009, sites were not visited prior to snowmelt.

Table S8: Difference in average bud break date from 2011 to 2015.

Plot	Species	2011	2015	2011-2015
PC01	ACCI	109	96	13
PC01	ACMA3	135	86	49
PC01	COLA3	89	74	15
PC01	LIBO3	95	68	27
PC01	PSME	154	129	25
PC01	RUUR	110	81	29
PC01	TROV2	89	77	12
PC01	TSHE	158	136	22
PC01	VAPA	99	70	29
PC01	VISE3	81	66	15
PC02	ACCI	109	82	27
PC02	CHUM	137	96	41
PC02	COLA3	102	77	25
PC02	CONU4	107	79	28
PC02	LIBO3	98	74	24
PC02	PSME	158	131	27
PC02	RHMA	153	144	9
PC02	RUUR	131	91	40
PC02	TROV2	92	76	16
PC02	TSHE	162	143	19
PC02	VAPA	96	70	26
PC02	VISE3	95	61	34
PC04	ACCI	103	NA	NA
PC04	COLA3	98	NA	NA
PC04	LIBO3	101	NA	NA
PC04	PSME	151	NA	NA
PC04	RHMA	153	NA	NA
PC04	RUUR	112	NA	NA
PC04	SYRE	90	NA	NA

PC04	TROV2	93	NA	NA
PC04	TSHE	157	NA	NA
PC04	VAPA	105	NA	NA
PC04	VISE3	85	NA	NA
PC05	ACCI	117	NA	NA
PC05	CONU4	102	NA	NA
PC05	LIBO3	102	NA	NA
PC05	PSME	158	NA	NA
PC05	RHMA	160	NA	NA
PC05	RUUR	119	NA	NA
PC05	TSHE	161	NA	NA
PC05	VAPA	110	NA	NA
PC05	VISE3	85	NA	NA
PC07	ACCI	122	95	27
PC07	CHUM	161	116	45
PC07	LIBO3	129	67	62
PC07	PSME	180	147	33
PC07	RHMA	170	142	28
PC07	TSHE	171	154	17
PC08	ACCI	112	NA	NA
PC08	CHUM	133	NA	NA
PC08	COLA3	102	NA	NA
PC08	LIBO3	113	NA	NA
PC08	PSME	166	NA	NA
PC08	RHMA	158	NA	NA
PC08	RUUR	130	NA	NA
PC08	SYRE	105	NA	NA
PC08	TROV2	98	NA	NA
PC08	TSHE	165	NA	NA
PC08	VAPA	108	NA	NA
PC08	VISE3	88	NA	NA
PC09	ABAM	174	149	25
PC09	ACCI	127	92	35
PC09	CHUM	169	117	52
PC09	COCA13	145	81	64
PC09	LIBO3	154	75	79
PC09	PSME	179	151	28
PC09	RHMA	179	144	35
PC09	RUUR	155	84	71
PC09	TROV2	137	91	46
PC09	TSHE	176	150	26
PC09	VAPA	138	74	64
PC09	**VISE3**	**144**	**59**	**85**

PC10	ABAM	177	NA	NA
PC10	ACCI	136	NA	NA
PC10	CHUM	154	NA	NA
PC10	COCA13	140	NA	NA
PC10	COLA3	130	NA	NA
PC10	LIBO3	129	NA	NA
PC10	PSME	173	NA	NA
PC10	RHMA	172	NA	NA
PC10	RUUR	146	NA	NA
PC10	TSHE	172	NA	NA
PC10	VAPA	136	NA	NA
PC10	VISE3	119	NA	NA
PC11	ABPR	174	NA	NA
PC11	ACCI	133	NA	NA
PC11	CHUM	157	NA	NA
PC11	COCA13	147	NA	NA
PC11	LIBO3	136	NA	NA
PC11	PSME	179	NA	NA
PC11	RUUR	162	NA	NA
PC11	SYRE	144	NA	NA
PC11	TROV2	137	NA	NA
PC11	TSHE	173	NA	NA
PC11	VAPA	138	NA	NA
PC11	VISE3	133	NA	NA
PC12	ACCI	130	88	42
PC12	CHUM	150	110	40
PC12	COLA3	137	73	64
PC12	LIBO3	131	66	65
PC12	PSME	178	147	31
PC12	RUUR	152	70	82
PC12	SYRE	137	56	81
PC12	TROV2	132	89	43
PC12	TSHE	173	150	23
PC12	VAPA	131	67	64
PC12	VISE3	133	60	73
PC13	ABAM	181	NA	NA
PC13	ACCI	141	NA	NA
PC13	CHUM	172	NA	NA
PC13	COCA13	165	NA	NA
PC13	LIBO3	164	NA	NA
PC13	PSME	186	NA	NA
PC13	RUUR	175	NA	NA
PC13	TSHE	183	NA	NA

PC13	VISE3	159	NA	NA
PC14	ACCI	139	NA	NA
PC14	CHUM	159	NA	NA
PC14	COCA13	140	NA	NA
PC14	COLA3	140	NA	NA
PC14	LIBO3	137	NA	NA
PC14	PSME	178	NA	NA
PC14	RHMA	177	NA	NA
PC14	RUUR	162	NA	NA
PC14	TROV2	130	NA	NA
PC14	TSHE	171	NA	NA
PC14	VAPA	138	NA	NA
PC14	VISE3	129	NA	NA
PC15	ABAM	179	151	28
PC15	ACCI	134	88	46
PC15	CHUM	152	103	49
PC15	COCA13	148	87	61
PC15	COLA3	130	81	49
PC15	LIBO3	138	67	71
PC15	PSME	179	147	32
PC15	RUUR	164	92	72
PC15	SYRE	137	68	69
PC15	TROV2	137	93	44
PC15	TSHE	175	148	27
PC15	VAPA	133	70	63
PC15	VISE3	130	54	76
PC16	ACCI	126	NA	NA
PC16	CHUM	150	NA	NA
PC16	LIBO3	127	NA	NA
PC16	PSME	175	NA	NA
PC16	RHMA	172	NA	NA
PC16	RUUR	154	NA	NA
PC16	TSHE	171	NA	NA
PC16	VAPA	133	NA	NA
PC16	VISE3	130	NA	NA
PC17	ABAM	181	151	30
PC17	ACCI	149	87	62
PC17	CHUM	190	132	58
PC17	COCA13	174	108	66
PC17	PSME	186	158	28
PC17	RUUR	186	113	73
PC17	TROV2	NA	118	NA
PC17	TSHE	186	152	34

PC17	VAME	NA	74	NA
PC17	VISE3	169	97	72
PC18	ABPR	181	NA	NA
PC18	ACCI	162	NA	NA
PC18	CHUM	191	NA	NA
PC18	COCA13	174	NA	NA
PC18	PSME	187	NA	NA
PC18	RUUR	179	NA	NA
PC18	TSHE	187	NA	NA
PC18	VISE3	172	NA	NA

Notes

Mean bud break from 2011 was subtracted from 2015 to find the most extreme advancement of bud break between those two years.

Table S9: Physical variables included in microclimate model

Plot	Elevation (m)	Slope (25m radius)	Aspect (25 m radius)	Relative topographic position (500 m radius)
PC001	489.47	61.484	0.917	109.852
PC002	478.21	21.826	0.480	76.648
PC004	487.25	66.114	-0.966	71.178
PC005	643.14	64.593	-0.983	184.431
PC007	899.88	14.373	0.425	222.997
PC008	646.51	48.223	-0.784	117.416
PC009	984.48	32.431	-0.214	149.310
PC010	983.62	18.496	-0.873	192.657
PC011	1114.83	28.690	-0.360	236.108
PC012	1083.18	39.696	-0.973	243.581
PC013	1177.89	18.772	-0.402	222.385
PC014	964.54	20.847	0.215	199.705
PC015	970.82	14.109	-0.541	196.015
PC016	1025.07	34.904	-0.924	265.403
PC017	1299.86	41.105	0.473	229.104
PC018	1329.72	45.493	-0.017	254.462

Table S10: Elevation as a predictor of bud break for each species and year.

Year	Species code	Adj R^2	P-value	F-stat	df1	df2	Intercept	Slope
2009	ABAM	0.83	1.99E-02	20.68	1	2	123.35	0.03
2010	ABAM	Not Sig	2.19E-01	2.40	1	2	0.00	0.00
2011	ABAM	Not Sig	1.48E-01	3.76	1	2	0.00	0.00
2012	ABAM	Not Sig	1.98E-01	2.72	1	2	0.00	0.00
2013	ABAM	Not Sig	8.44E-01	0.05	1	2	0.00	0.00
2014	ABAM	Not Sig	3.37E-01	1.30	1	2	0.00	0.00
2015	ABAM	Not Sig	6.91E-01	0.28	1	1	0.00	0.00
2016	ABAM	Not Sig	4.91E-01	0.61	1	2	0.00	0.00
2009	ACCI	0.82	4.61E-04	38.01	1	6	66.78	0.06
2010	ACCI	0.74	2.37E-05	40.88	1	3	76.61	0.03
2011	ACCI	0.86	1.22E-07	95.72	1	4	80.00	0.05
2012	ACCI	0.65	9.77E-05	28.91	1	4	94.24	0.03
2013	ACCI	0.67	7.14E-05	30.82	1	4	76.46	0.03
2014	ACCI	0.72	1.89E-05	39.96	1	4	71.22	0.02
2015	ACCI	Not Sig	8.76E-01	0.03	1	5	0.00	0.00
2016	ACCI	0.52	1.02E-03	17.07	1	4	74.38	0.02
2009	CHUM	0.72	3.19E-04	28.73	1	7	90.57	0.05
2010	CHUM	0.71	2.01E-04	29.70	1	8	88.36	0.06
2011	CHUM	0.69	2.64E-04	27.79	1	8	96.87	0.06
2012	CHUM	0.74	1.07E-04	34.52	1	8	91.44	0.06
2013	CHUM	0.68	3.06E-04	26.78	1	8	88.10	0.05
2014	CHUM	0.51	3.59E-03	13.58	1	8	81.96	0.04
2015	CHUM	0.61	4.06E-02	8.89	1	9	75.81	0.04
2016	CHUM	Not Sig	2.14E-01	1.74	1	8	0.00	0.00
2009	COCA	Not Sig	4.29E-01	0.83	1	2	0.00	0.00
2010	COCA	0.81	1.34E-03	31.71	1	10	4.83	0.11
2011	COCA	0.89	2.68E-04	57.94	1	10	53.35	0.09
2012	COCA	0.77	2.66E-03	24.20	1	10	66.43	0.07
2013	COCA	0.92	1.00E-04	82.47	1	10	47.10	0.07
2014	COCA	Not Sig	1.80E-01	2.30	1	10	0.00	0.00
2015	COCA	Not Sig	1.60E-01	15.17	1	1	0.00	0.00

2016	COCA	0.78	2.35E-03	25.44	1	10	42.06	0.06
2009	COLA	Not Sig	4.33E-01	1.53	1	1	0.00	0.00
2010	COLA	0.52	4.08E-02	7.50	1	5	67.45	0.04
2011	COLA	0.91	1.64E-04	69.20	1	10	59.60	0.07
2012	COLA	0.71	5.48E-03	17.91	1	10	86.57	0.03
2013	COLA	0.96	1.72E-05	152.61	1	10	64.61	0.05
2014	COLA	0.65	9.62E-03	13.99	1	10	64.41	0.03
2015	COLA	Not Sig	8.98E-01	0.02	1	11	0.00	0.00
2016	COLA	0.44	4.40E-02	6.46	1	10	61.96	0.03
2009	LIBO	Not Sig	9.25E-02	4.85	1	9	0.00	0.00
2010	LIBO	0.44	5.54E-03	11.38	1	12	52.25	0.05
2011	LIBO	0.80	9.04E-06	53.80	1	12	60.40	0.08
2012	LIBO	0.73	5.48E-05	36.99	1	12	93.02	0.04
2013	LIBO	0.80	8.93E-06	53.93	1	12	60.30	0.06
2014	LIBO	0.77	2.55E-05	43.53	1	12	62.59	0.03
2015	LIBO	Not Sig	5.46E-01	0.43	1	9	0.00	0.00
2016	LIBO	0.63	3.98E-04	23.53	1	12	46.40	0.03
2009	PSME	0.88	1.18E-02	30.38	1	2	121.87	0.03
2010	PSME	0.86	4.99E-07	83.72	1	3	125.57	0.05
2011	PSME	0.90	1.36E-08	135.87	1	4	136.52	0.04
2012	PSME	0.71	2.65E-05	37.45	1	4	128.15	0.03
2013	PSME	0.81	1.51E-06	62.94	1	4	111.08	0.03
2014	PSME	0.73	1.38E-05	42.38	1	4	118.31	0.03
2015	PSME	0.94	2.34E-04	87.73	1	5	114.31	0.03
2016	PSME	0.71	2.48E-05	37.95	1	4	112.21	0.03
2009	RHMA	0.77	1.21E-03	27.38	1	6	132.82	0.02
2010	RHMA	0.75	1.56E-03	25.02	1	6	126.52	0.04
2011	RHMA	0.92	3.23E-05	88.22	1	6	131.83	0.04
2012	RHMA	Not Sig	5.70E-02	5.18	1	6	0.00	0.00
2013	RHMA	0.42	3.62E-02	6.69	1	6	125.40	0.02
2014	RHMA	0.65	5.56E-03	15.57	1	6	118.88	0.02
2015	RHMA	Not Sig	7.67E-01	0.15	1	1	0.00	0.00
2016	RHMA	Not Sig	5.46E-02	5.31	1	6	0.00	0.00
2009	RUUR	0.44	4.34E-02	6.51	1	10	119.15	0.02

2010	RUUR	0.76	1.49E-05	44.76	1	3	64.71	0.07
2011	RUUR	0.89	1.08E-07	109.15	1	3	78.04	0.08
2012	RUUR	0.79	6.32E-06	52.77	1	3	94.73	0.05
2013	RUUR	0.83	1.71E-06	67.22	1	3	67.38	0.06
2014	RUUR	0.71	4.50E-05	35.91	1	3	64.38	0.04
2015	RUUR	Not Sig	5.00E-01	0.55	1	9	0.00	0.00
2016	RUUR	0.72	3.59E-05	37.60	1	3	65.02	0.05
2009	SYRE	Not Sig					0.00	
2010	SYRE	Not Sig	5.64E-02	9.17	1	2	0.00	0.00
2011	SYRE	0.97	1.28E-03	141.62	1	2	50.31	0.08
2012	SYRE	Not Sig	6.49E-02	8.14	1	2	0.00	0.00
2013	SYRE	0.76	3.52E-02	13.42	1	2	65.44	0.04
2014	SYRE	Not Sig	1.44E-01	3.88	1	2	0.00	0.00
2016	SYRE	Not Sig	1.64E-01	3.37	1	2	0.00	0.00
2009	TROV	Not Sig					0.00	
2010	TROV	0.92	2.42E-05	96.37	1	6	41.68	0.06
2011	TROV	0.94	8.66E-06	131.32	1	6	52.35	0.08
2012	TROV	0.95	1.29E-04	112.57	1	5	63.68	0.06
2013	TROV	0.90	5.35E-06	90.74	1	13	58.88	0.05
2014	TROV	0.83	8.31E-06	60.83	1	8	54.74	0.04
2015	TROV	0.75	1.57E-02	16.25	1	9	54.35	0.04
2016	TROV	0.88	1.15E-06	91.49	1	8	59.71	0.04
2009	TSHE	0.59	1.22E-03	18.62	1	8	133.90	0.02
2010	TSHE	0.79	2.96E-06	55.98	1	4	140.89	0.03
2011	TSHE	0.90	1.32E-08	136.43	1	4	143.07	0.03
2012	TSHE	0.71	2.55E-05	37.74	1	4	144.65	0.02
2013	TSHE	0.61	2.22E-04	24.29	1	4	139.02	0.02
2014	TSHE	0.59	3.20E-04	22.41	1	4	131.39	0.02
2015	TSHE	0.60	2.55E-02	9.91	1	5	132.88	0.02
2016	TSHE	0.51	1.19E-03	16.41	1	4	129.38	0.02
2009	VAPA	Not Sig					0.00	
2010	VAPA	0.75	7.92E-04	27.37	1	14	61.49	0.04
2011	VAPA	0.93	3.56E-07	138.08	1	7	68.81	0.06
2012	VAPA	0.56	2.93E-03	15.26	1	7	92.07	0.03

2013	VAPA	0.67	6.68E-04	23.55	1	7	65.11	0.04
2014	VAPA	0.80	4.84E-05	46.02	1	7	58.44	0.03
2015	VAPA	Not Sig	9.52E-01	0.00	1	2	0.00	0.00
2016	VAPA	Not Sig	9.01E-02	3.52	1	7	0.00	0.00
2009	VISE	0.78	9.47E-04	29.80	1	6	72.42	0.05
2010	VISE	0.56	2.00E-03	16.19	1	8	35.23	0.07
2011	VISE	0.91	2.51E-08	139.65	1	3	31.21	0.10
2012	VISE	0.90	4.06E-08	128.85	1	3	37.08	0.08
2013	VISE	0.76	1.50E-05	44.74	1	3	46.82	0.06
2014	VISE	0.35	1.21E-02	8.49	1	3	49.21	0.04
2015	VISE	Not Sig	3.55E-01	1.09	1	9	0.00	0.00
2016	VISE	0.69	7.20E-05	32.58	1	3	27.61	0.06

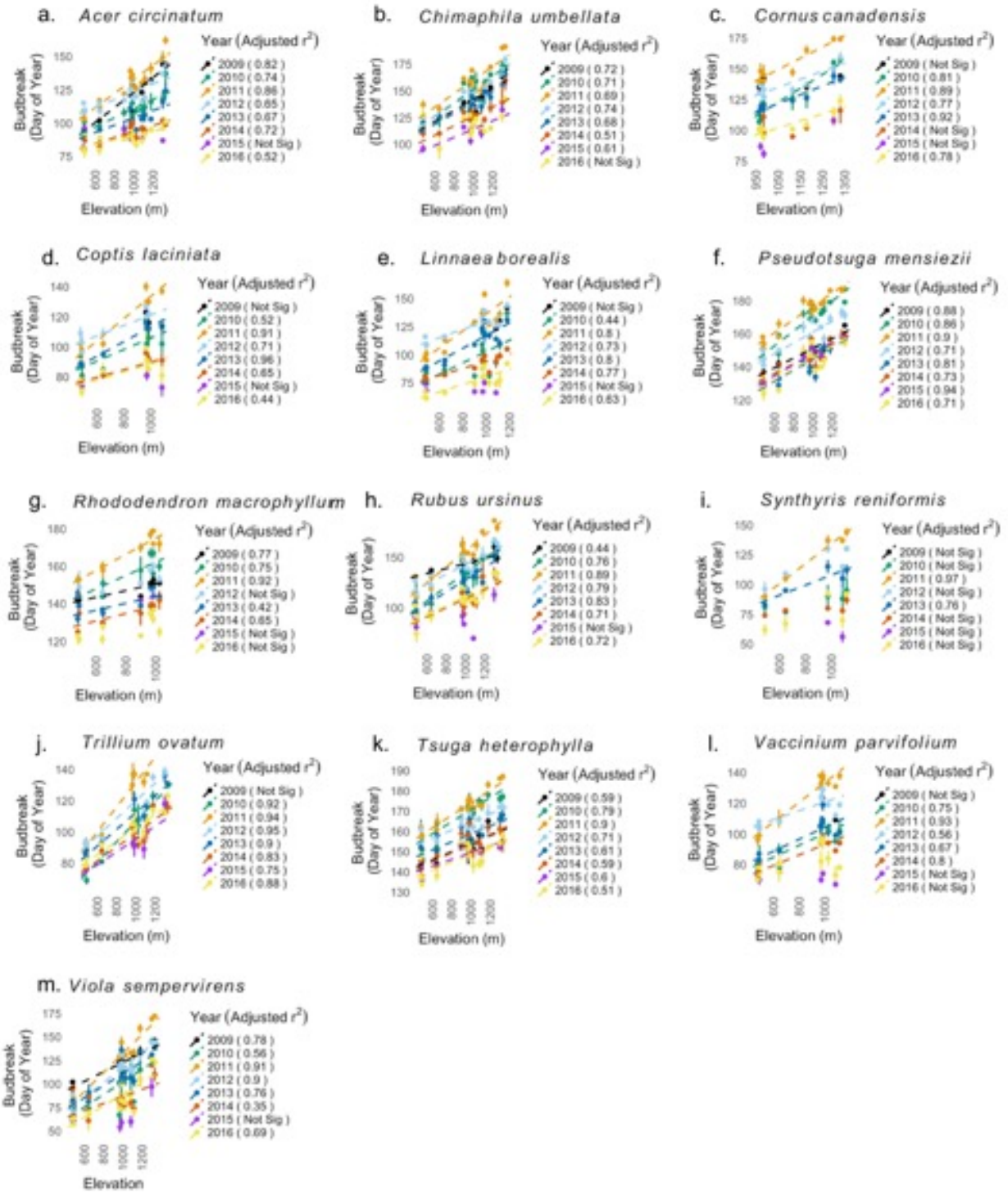

Figure S1: Elevation as a predictor of bud break for focal species from 2009-2016. Colors represent year, while dashed line is the line of best fit. Error bars are ± SE. *Abies amabalis, Abies procera, Acer macrophyllum, Cornus nuttallii* and *Vaccinium membranaceum* are not included due to limited distribution and small sample sizes.

APPENDIX B

APPENDIX S2

Table S1: Location data of phenology sites

Site Code	Site Type	UTM X (m, zone 10)	UTM Y (m, zone 10)	Latitude (dd.mmss)	Longitude (dd.mmss)	Elevation (m)
PC01	PC	559337.35	4895046.44	44.2062254	-122.25732	489
PC02	PC	560002.77	4896020.61	44.2149409	-122.24888	478
PC04	PC	559036.61	4896294.35	44.2174841	-122.26094	487
PC05	PC	559285.46	4896520.5	44.2194998	-122.2578	643
PC07	PC	563676.24	4896880.81	44.222373	-122.20279	900
PC08	PC	564602.71	4898330.95	44.2353459	-122.19102	647
PC09	PC	570158.63	4897484.72	44.2272141	-122.12156	985
PC10	PC	568428.4	4899050.06	44.2414701	-122.14302	984
PC11	PC	567818.24	4900020.42	44.2502624	-122.15054	1115
PC12	PC	567119.53	4899576.57	44.2463316	-122.15934	1083
PC13	PC	568962.13	4899919.42	44.2492458	-122.13622	1178
PC14	PC	567112.4	4900996.98	44.259119	-122.15925	965
PC15	PC	566249.07	4901763.91	44.2661021	-122.16997	971
PC16	PC	565638.52	4901903.32	44.2674124	-122.1776	1025
PC17	PC	568878.06	4902587.96	44.2732761	-122.13692	1300
PC18	PC	569001.89	4902746.4	44.2746907	-122.13535	1330
DT	DT	560008.19	4896195.93	44.216519	-122.24879	436

Table S2 Regression equations used to fill in any missing or erroneous temperature data.

Site	Equation	Adjusted R^2	df	F-stat	P-value
PC01	PC01 = RS02 x 0.941 + 0.649	0.989	1,45215	425924	***
PC02	PC02 = CS2met x 0.933 + 1.074	0.986	1,49115	354185	***
PC04	PC04 = RS89 x 0.985 + 0.632	0.994	1,54915	979041	***
PC05	PC05 = RS86 x 0.992 + 0.430	0.994	1,44049	706341	***
PC07	PC07 = RS05 x 0.987 - 0.075	0.996	1,55057	1271158	***
PC08	PC08 = RS10 x 1.000 + 0.115	0.997	1,54568	1571495	***
PC09	PC09 = RS12 x 1.001 + 0.381	0.992	1,53536	647952	***
PC10	PC10 = RS05 x 1.003 - 0.568	0.986	1,54745	376250	***
PC11	PC11 = RS26 x 0.975 - 0.554	0.991	1,47045	495211	***
PC12	PC12 = RS26 x 0.979 + 0.107	0.996	1,54593	1402571	***
PC13	PC13 = RS26 x 0.952 - 1.235	0.971	1,54196	181439	***
PC14	PC14 = RS05 x 1.016 - 0.454	0.989	1,55067	485521	***
PC15	PC15 = HI15 x 0.984 + 0.386	0.985	1,48635	320198	***
PC16	PC16 = RS26 x 0.996 - 0.026	0.986	1,54059	372480	***
PC17	PC17 = RS04 x 0.977 + 0.014	0.992	1,47550	595117	***
PC18	PC18 = RS04 x 1.001 - 0.203	0.984	1,48787	308451	***

Notes

-- Non Significant; * P<0.05; ** P<0.01; ***P<0.001; In the site column, PC represents "phenology core"; In the equation column, all
abbeviations following = are representative of reference stands (RS) or other climate stations (HI15 and CS2met); df, degrees of freedom.

Table S3: Alternative and selected bud break models tested; final models in bold:

Species	Model	CP	Adj R^2
Acer circinatum	**log(Budbreak)~ meanaprtemp + log(apr_chill.force)**	**0.17**	**0.74**
Acer circinatum	log(Budbreak) ~ meanaprtemp + sqrt(days_below_0) + sqrt(DOYchilling_above_1200)	2.09	0.74
Acer circinatum	log(Budbreak) ~ meanaprtemp + sqrt(days_below_0)	5.25	0.70
Pseudotsuga menziesii	Budbreak ~ meanaprtemp + juneforce + lastdoybelow0	6.5	0.85
Pseudotsuga menziesii	Budbreak ~ juneforce	25.55	0.85
Pseudotsuga menziesii	**Budbreak ~ june_chill.force**	**18.55**	**0.83**
Vaccinium parvifolium	sqrt(Budbreak)~ scale(obs_aprsnow) + scale(lastdoybelow0) + scale(meanaprtemp) + scale(sqrt(may_chill.force)) + scale(obs_aprsnow)*scale(sqrt(may_chill.force)	4.73	0.82
Vaccinium parvifolium	**sqrt(Budbreak)~ scale(lastdoybelow0) + scale(meanaprtemp) + scale(log(apr_chill.force)**	**0.09**	**0.81**
Vaccinium parvifolium	sqrt(Budbreak)~ scale(obs_aprsnow) + scale(lastdoybelow0) + scale(sqrt(mayforce)) + (obs_aprsnow)*scale(sqrt(mayforce)	2.69	0.78

Vaccinium parvifolium	sqrt(Budbreak)~ scale(sqrt(days_below_0) + scale(meanaprtemp) + scale(log(aprforce)	2.11	0.76
Trillium ovatum	**sqrt(Budbreak) ~ (obs_aprsnow) + (sqrt(days_below_0)) + (meanaprtemp)**	**5.42**	**0.85**
Trillium ovatum	sqrt(Budbreak) ~ scale(sqrt(days_below_0)) + scale(obs_aprsnow) + scale(lastdoybelow0) + scale(meanaprtemp) + scale(sqrt(may_chill.force)) + scale(sqrt(may_chill.force)) * scale(obs_aprsnow)	6.42	0.86
Trillium ovatum	sqrt(Budbreak) ~ scale(sqrt(days_below_0)) + scale(obs_aprsnow) + scale(lastdoybelow0) + scale(meanaprtemp) + scale(log(apr_chill.force)) + scale(log(apr_chill.force)) * scale(obs_aprsnow)	6.09	0.86

Table S4: Difference in observed and predicted bud break days.

SITECODE[+]	Year	Species[++]	Observed budbreak	Predicted budbreak	Difference (Days)	Elevation (m)
DiscTrail	2014	ACCI	89	89.53	-0.40	436
DiscTrail	2015	ACCI	88	86.29	1.43	436
DiscTrail	2016	ACCI	80	79.06	0.99	436
PC02	2017	ACCI	84	92.00	-8.00	478
PC01	2017	ACCI	89	89.69	-0.69	489
PC05	2017	ACCI	91	90.86	0.14	643
PC08	2017	ACCI	95	94.92	0.08	647
PC07	2017	ACCI	99	103.07	-4.07	900
PC14	2017	ACCI	104	106.87	-2.87	965
PC15	2017	ACCI	100	104.73	-4.73	971
PC10	2017	ACCI	102	105.79	-3.79	984
PC09	2017	ACCI	106	110.65	-4.65	985
PC16	2017	ACCI	87	104.35	-17.35	1025
PC12	2017	ACCI	105	105.39	-0.39	1083
PC11	2017	ACCI	101	109.76	-8.76	1115
PC13	2017	ACCI	115	118.28	-3.28	1178
PC17	2017	ACCI	137	120.92	16.08	1300
PC18	2017	ACCI	140	122.36	17.64	1330
PC02	2017	PSME	140	148.89	-8.89	478

PC01	2017	PSME	137	143.44	-6.44	489
PC05	2017	PSME	138	140.26	-2.26	643
PC08	2017	PSME	147	147.55	-0.55	647
PC07	2017	PSME	152	156.31	-4.31	900
PC14	2017	PSME	155	156.85	-1.85	965
PC15	2017	PSME	158	154.91	3.09	971
PC10	2017	PSME	159	157.52	1.48	984
PC09	2017	PSME	158	163.17	-5.17	985
PC16	2017	PSME	147	152.35	-5.35	1025
PC12	2017	PSME	152	153.81	-1.81	1083
PC11	2017	PSME	157	156.79	0.21	1115
PC13	2017	PSME	161	165.13	-4.13	1178
PC17	2017	PSME	166	168.04	-2.04	1300
PC18	2017	PSME	168	168.70	-0.70	1330
DiscTrail	2014	TROV2	88	84.62	3.38	436
DiscTrail	2015	TROV2	84	75.34	8.32	436
DiscTrail	2016	TROV2	86	73.21	12.79	436
PC02	2017	TROV2	86	89.22	-3.22	478
PC01	2017	TROV2	82	86.73	-4.73	489
PC08	2017	TROV2	95	92.56	2.44	647
PC14	2017	TROV2	113	112.11	0.89	965
PC15	2017	TROV2	105	109.14	-4.14	971
PC09	2017	TROV2	115	113.58	1.42	985
PC16	2017	TROV2	113	102.35	10.65	1025
PC12	2017	TROV2	105	102.31	2.69	1083
PC11	2017	TROV2	118	107.09	10.91	1115
PC13	2017	TROV2	130	122.41	7.59	1178
PC17	2017	TROV2	144	127.03	16.97	1300
PC18	2017	TROV2	146	128.55	17.45	1330
DiscTrail	2014	VAPA	88	79.14	8.86	436
DiscTrail	2015	VAPA	84	70.19	13.31	436
DiscTrail	2016	VAPA	71	66.47	4.33	436
PC02	2017	VAPA	78	92.39	-14.39	478
PC01	2017	VAPA	79	83.23	-4.23	489

PC05	2017	VAPA	88	85.36	2.64	643
PC08	2017	VAPA	87	92.35	-5.35	647
PC14	2017	VAPA	115	117.09	-2.09	965
PC15	2017	VAPA	102	115.71	-13.71	971
PC10	2017	VAPA	108	102.14	5.86	984
PC09	2017	VAPA	116	122.99	-6.99	985
PC16	2017	VAPA	96	101.96	-5.96	1025
PC12	2017	VAPA	91	103.36	-12.36	1083
PC11	2017	VAPA	110	107.87	2.13	1115

+PC = phenology core; DiscTrail = discovery trail

++ACCI = *Acer circinatum;* PSME = *Pseudotsuga menziesii*; TROV2 = *Trillium ovatum*; VAPA = *Vaccinium parvifolium*

TABLE S5: Variables initially included in microclimate models.

Microclimate variable	Predictor variables in initial models
April chilling after forcing	sqrt(apr_chill.force) ~ ELEVATION + tpi_500m + aspect +sqrt(biomass) + vegheight + Nov_Mar_acindex +Slope + mean_mar_temp_PRIMET
DOY chilling above 1200	sqrt(DOYchilling_above_1200) ~ ELEVATION + aspect +sqrt(biomass) + vegheight + Nov_Mar _acindex +Slope + mean_mar_temp_PRIMET
Mean april tempearture	meanaprtemp ~ ELEVATION +tpi_500m + aspect +sqrt(biomass) + vegheight + (Nov_Mar_acindex) + mean_apr_temp_PRIMET + Slope
Days below 0	sqrt(days_below_0) ~ ELEVATION +tpi_500m + sqrt(biomass) + (Nov_May_acindex) + Slope + mean_temp_novmay_PRIMET
Last day of year below 0	lastdoybelow0) ~ ELEVATION +tpi_500m + aspect +sqrt(biomass) + (Nov_May_acindex) + mean_temp_novmay_PRIMET+ Slope
June forcing after chilling	sqrt(jun_chill.force) ~ ELEVATION +tpi_500m + aspect + sqrt(biomass) + vegheight + (Nov_May_acindex) + Slope + meantemp_mar_may_PRIMET
April 1 snow	snow_present ~ log(biomass) + ELEVATION + sqrt(CENMET_snowdepth) +sqrt(UPLMET_snowdepth) + hja_aspect + avg_monthly_airtemp_PRIMET + avg_monthly_airtmep_UPLMET

Table S6: Model summaries of microclimate predictions.

Microclimate variable	Predictor variables	F-stat$_{(df)}$	R^2	p-value
April chilling after forcing	ELEVATION + tpi_500m + sqrt(biomass) + Nov_Mar_acindex + Slope + mean_mar_temp_PRIMET	$72.3_{(6,121)}$	0.78	***
DOY chilling above 1200	Elevation + Nov_Mar_acindex	$117.8_{(2,125)}$	0.65	***
Mean april tempearture	Elevation + tpi_500m + meanapriltemp_PRIMET + Slope	$464.4_{(4,123)}$	0.94	***
Days below 0	Elevation + tpi_500m + mean_temp_Nov-May_PRIMET	$138.9_{(3,124)}$	0.77	***
Last day of year below 0	Elevation + mean_temp_Nov-May_PRIMET	$169.9_{(2,125)}$	0.731	***
June forcing after chilling	Elevation +tpi_500m +sqrt(biomass) + Nov_May_acidex + Slope + mean_temp_Mar-May_PRIMET	$177.8_{(6,121)}$	0.90	***
April 1 snow	log(biomass) + ELEVATION + sqrt(CENMET_snowdepth) + avgUPLMET_airtemp	G2: 0.98 Deviance: 1105. 326 Dispersion: 0.91		

Table S7: Observed presence absence of April 1 snow versus predicted probability.

Month	Mean	SD	Min	Max	Observations (n)
April absent	0.27	0.25	0.02	0.89	51
April present	0.64	0.29	0.08	0.98	77

Table S8: Landscape model predictions of observed 2009 to 2016 bud break

Species	R_2	F-stat$_{(df)}$	p-value
Acer circinatum	0.60	$164.3_{(1,109)}$	***
Pseudotsuga menziesii	0.84	$538.9_{(1,105)}$	***
Trillium ovatum	0.62	$109.9_{(1,66)}$	***
Vaccinium parvifolium	0.19	$17.79_{(1,75)}$	***

Figure S1

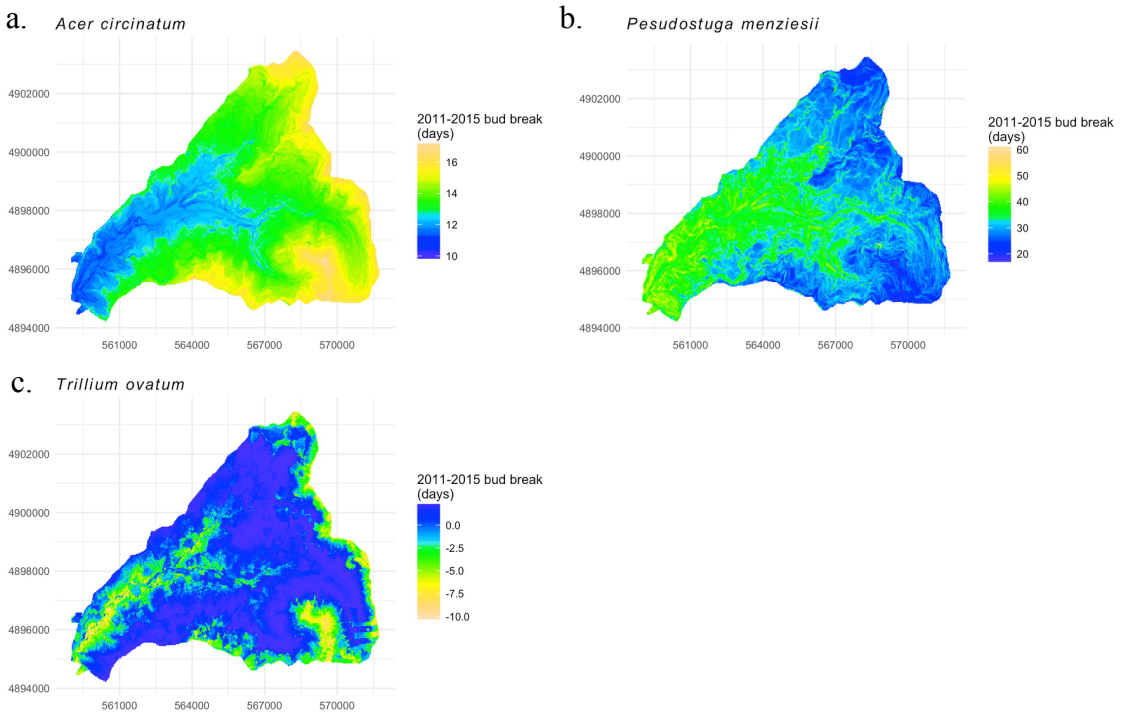

Figure 3: Range predicted bud break across the andrews Andrews between the warmest (2015) and coolest (2011) years in the phenology record. (a) *Acer circinatum* (b) *Pseudotsuga menziesii* (c) *Trillium ovatum.* Colors represent the range between 2011 and 2015 values (2015 was the warmest year in the phenology record while 2011 was the coolest). Blues represent regions with the least range bud break, while yellows are the areas with the greatest range between the two years. Greens are intermediate. Red huckleberry is not presented due to limited accuracy of the landscape model

APPENDIX C

APPENDIX S3

Auguie B (2017). _gridExtra: Miscellaneous Functions for "Grid" Graphics_. R package version 2.3, <URL: https://CRAN.R-project.org/package=gridExtra>.

Fox J and Weisberg S (2011). _An R Companion to Applied Regression_, Second edition. Sage, Thousand Oaks CA. <URL:http://socserv.socsci.mcmaster.ca/jfox/Books/Companion>.

Hope RM (2013). _Rmisc: Rmisc: Ryan Miscellaneous_. R package version 1.5, <URL: https://CRAN.R-project.org/package=Rmisc>.

Miller TLboFcbA (2017). _leaps: Regression Subset Selection_. R package version 3.0, <URL: https://CRAN.R-project.org/package=leaps>.

Oksanen J, Blanchet FG, Friendly M, Kindt R, Legendre P, McGlinn D, Minchin PR, O'Hara RB, Simpson GL, Solymos P, Stevens MHH, Szoecs E and Wagner H (2017). _vegan: Community Ecology Package_. R package version 2.4-4, <URL:https://CRAN.R-project.org/package=vegan>.

Oswaldo Santos Baquero (2017). ggsn: North Symbols and Scale Bars for Maps Created with 'ggplot2' or 'ggmap'. R package version 0.4.0. https://CRAN.R-project.org/package=ggsn

R Core Team (2017). _R: A Language and Environment for Statistical Computing_. R Foundation for Statistical Computing, Vienna, Austria. <URL: https://www.R-project.org/>.

RStudio Team (2016). _RStudio: Integrated Development Environment for R_. RStudio, Inc.,Boston, MA. <URL: http://www.rstudio.com/>.

Richard A. Becker, Allan R. Wilks. R version by Ray Brownrigg. Enhancements by Thomas P Minka and Alex Deckmyn. (2017). maps: Draw Geographical Maps. Rpackage version 3.2.0. https://CRAN.R-project.org/package=maps

Robert J. Hijmans (2017). raster: Geographic Data Analysis and Modeling. R package version 2.6-7. https://CRAN.R-project.org/package=raster

Roger Bivand, Tim Keitt and Barry Rowlingson (2017). rgdal: Bindings for the 'Geospatial' Data Abstraction Library. R package version 1.2-16. https://CRAN.R-project.org/package=rgdal

Sarkar D (2008). _Lattice: Multivariate Data Visualization with R_. Springer, New York. ISBN 978-0-387-75968-5, <URL: http://lmdvr.r-forge.r-project.org>.

Simpson G (2016). _permute: Functions for Generating Restricted Permutations of Data_. R package version 0.9-4, <URL: https://CRAN.R-project.org/package=permute>.

Venables WN and Ripley BD (2002). _Modern Applied Statistics with S_, Fourth edition. Springer, New York. ISBN 0-387-95457-0, <URL: http://www.stats.ox.ac.uk/pub/MASS4>.

Vu VQ (2011). _ggbiplot: A ggplot2 based biplot_. R package version 0.55, <URL: http://github.com/vqv/ggbiplot>.

Wickham H (2017). _scales: Scale Functions for Visualization_. R package version 0.5.0, <URL:https://CRAN.R-project.org/package=scales>.

Wickham H and Chang W (2017). _devtools: Tools to Make Developing R Packages Easier_. R package version 1.13.3, <URL: https://CRAN.R-project.org/package=devtools>.

Wickham H (2009). _ggplot2: Elegant Graphics for Data Analysis_.Springer-Verlag New York. ISBN 978-0-387-98140-6, <URL:http://ggplot2.org>.

Wickham H (2011). "The Split-Apply-Combine Strategy for Data Analysis." _Journal of Statistical Software_, *40*(1), pp. 1-29. <URL: http://www.jstatsoft.org/v40/i01/>.

REFERENCES CITED

Agee, J. K., and J. Kertis. 1987. Forest types of the North Cascades National Park Service Complex. Canadian Journal of Botany 65:1520–1530.

Bailey, J. D., and C. A. Harrington. 2006. Temperature regulation of bud-burst phenology within and among years in a young Douglas-fir (*Pseudotsuga menziesii*) plantation in western Washington, USA. Tree Physiology 26:421–430.

Bennie, J., E. Kubin, A. Wiltshire, B. Huntley, and R. Baxter. 2010. Predicting spatial and temporal patterns of bud-burst and spring frost risk in north-west Europe: the implications of local adaptation to climate. Global Change Biology 16:1503–1514.

Both, C., C. A. M. V. Turnhout, R. G. Bijlsma, H. Siepel, A. J. V. Strien, and R. P. B. Foppen. 2009. Avian population consequences of climate change are most severe for long-distance migrants in seasonal habitats. Proceedings of the Royal Society of London B: Biological Sciences:rspb20091525.

Brockway, D., C. Topik, M. Hemstrom, and W. Emmingham. 1983. Plant association and management guide for the Pacific silver fir zone: Gifford Pinchot National Forest.

Brown, G. W. 1969. Predicting Temperatures of Small Streams. Water Resources Research 5:68–75.

Buitenwerf, R., L. Rose, and S. I. Higgins. 2015. Three decades of multi-dimensional change in global leaf phenology. Nature Climate Change 5:364–368.

Chapin III, F. S., E Schulze, and H. A. Mooney. 1990. The ecology and economics of storage in plants. Annual Review of Ecology and Systematics 21:423–447.

Chuine, I., G. Cambon, and P. Comtois. 2000. Scaling phenology from the local to the regional level: advances from species-specific phenological models. Global Change Biology 6:943–952.

Chuine, I., P. Cour, and D. D. Rousseau. 1998. Fitting models predicting dates of flowering of temperate-zone trees using simulated annealing. Plant Cell and Environment 21:455–466.

Cleland, E. E., I. Chuine, A. Menzel, H. A. Mooney, and M. D. Schwartz. 2007. Shifting plant phenology in response to global change. Trends in Ecology & Evolution 22:357–365.

Daly, C., D. R. Conklin, and M. H. Unsworth. 2010. Local atmospheric decoupling in complex topography alters climate change impacts. International Journal of Climatology 30:1857–1864.

Daly, C., and W. McKee. 2016a, March 15. Air and soil temperature data from the Reference Stand network at the Andrews Experimental Forest, 1971 to present.

Daly, C., and W. McKee. 2016b, October. Meteorological data from benchmark stations at the Andrews Experimental Forest, 1957 to present.

Dobrowski, S. Z. 2011. A climatic basis for microrefugia: the influence of terrain on climate. Global Change Biology 17:1022–1035.

Ellis, T. M., and M. G. Betts. 2011. Bird abundance and diversity across a hardwood gradient within early seral plantation forest. Forest Ecology and Management 261:1372–1381.

Fitter, A. H., R. S. R. Fitter, I. T. B. Harris, and M. H. Williamson. 1995. Relationships between first flowering date and temperature in the flora of a locality in central England. Functional Ecology 9:55–60.

Forrest, J. R. K., and J. D. Thomson. 2011. An examination of synchrony between insect emergence and flowering in Rocky Mountain meadows. Ecological Monographs 81:469–491.

Franklin, J. 2017. Long-term growth, mortality and regeneration of trees in permanent vegetation plots in the Pacific Northwest, 1910 to present.

Franklin, J., F. W. Davis, M. Ikegami, A. D. Syphard, L. E. Flint, A. L. Flint, and L. Hannah. 2013. Modeling plant species distributions under future climates: how fine scale do climate projections need to be? Global Change Biology 19:473–483.

Frenne, P. D., F. Rodríguez-Sánchez, D. A. Coomes, L. Baeten, G. Verstraeten, M. Vellend, M. Bernhardt-Römermann, C. D. Brown, J. Brunet, J. Cornelis, G. M. Decocq, H. Dierschke, O. Eriksson, F. S. Gilliam, R. Hédl, T. Heinken, M. Hermy, P. Hommel, M. A. Jenkins, D. L. Kelly, K. J. Kirby, F. J. G. Mitchell, T. Naaf, M. Newman, G. Peterken, P. Petřík, J. Schultz, G. Sonnier, H. V. Calster, D. M. Waller, G.-R. Walther, P. S. White, K. D. Woods, M. Wulf, B. J. Graae, and K. Verheyen. 2013. Microclimate moderates plant responses to macroclimate warming. Proceedings of the National Academy of Sciences 110:18561–18565.

Frey, S. J. K., A. S. Hadley, and M. G. Betts. 2016a. Microclimate predicts within-season distribution dynamics of montane forest birds. Diversity and Distributions 22:944–959.

Frey, S. J. K., A. S. Hadley, S. L. Johnson, M. Schulze, J. A. Jones, and M. G. Betts. 2016b. Spatial models reveal the microclimatic buffering capacity of old-growth forests. Science Advances 2:e1501392.

Gaudry, W., S. Saïd, J.-M. Gaillard, T. Chevrier, A. Loison, D. Maillard, and C. Bonenfant. 2015. Partial migration or just habitat selection? Seasonal movements of roe deer in an Alpine population. Journal of Mammalogy 96:502–510.

Gholz, H. L., F. K. Fitz, and R. H. Waring. 1976. Leaf area differences associated with old-growth forest communities in the western Oregon Cascades. Canadian Journal of Forest Research 6:49–57.

Grimm, N. B., P. Groffman, M. Staudinger, and H. Tallis. 2016. Climate change impacts on ecosystems and ecosystem services in the United States: process and prospects for sustained assessment. Climatic Change 135:97–109.

Hagar, J. C. 2007. Wildlife species associated with non-coniferous vegetation in Pacific Northwest conifer forests: A review. Forest Ecology and Management 246:108–122.

Hänninen, H. 1995. Effects of climatic change on trees from cool and temperate regions: an ecophysiological approach to modelling of bud burst phenology. Canadian Journal of Botany 73:183–199.

Harmon, M., and K. O'Connell. 2015. Plant biomass dynamics following logging, burning, and thinning in Watersheds 6 and 7, Andrews Experimental Forest, 1979 to present.

Harrington, R., I. Woiwod, and T. Sparks. 1999. Climate change and trophic interactions. Trends in Ecology & Evolution 14:146–150.

Heide, O. M. 1993. Daylength and thermal time responses of budburst during dormancy release in some northern deciduous trees. Physiologia Plantarum 88:531–540.

Hwang, T., C. Song, J. M. Vose, and L. E. Band. 2011. Topography-mediated controls on local vegetation phenology estimated from MODIS vegetation index. Landscape Ecology 26:541–556.

Inouye, D. W. 2008. Effects of climate change on phenology, frost damage, and floral abundance of montane wildflowers. Ecology 89:353–362.

IPCC. 2007. Climate Change 2007 - The physical science basis: working group I contribution to the fourth assessment report of the IPCC. Cambridge University Press.

IPCC. 2014. Climate Change 2014: synthesis report. contribution of working groups I, II and III to the fifth assessment report of the Intergovernmental Panel on Climate Change. Geneva, Switzerland.

Johnson, S., and S. Gregory. 2016. Stream and air temperature data from stream gages and stream confluences in the Andrews Experimental Forest, 1950 to present.

Johnson, S., and S. Hadley. 2017. Air temperature at core phenology sites and additional bird monitoring sites in the Andrews Experimental Forest, 2009-Present.

Johnson, S., and J. Rothacher. 2016. Stream discharge in gaged watersheds at the Andrews Experimental Forest, 1949 to present. Long-Term Ecological Research.

Kerns, B. K., S. J. Alexander, and J. D. Bailey. 2004. Huckleberry abundance, stand conditions, and use in Western Oregon: evaluating the role of forest management. Economic Botany 58:668–678.

Körner, C., J. Paulsen, and E. M. Spehn. 2011. A definition of mountains and their bioclimatic belts for global comparisons of biodiversity data. Alpine Botany 121:73.

Kramer, K. 1994. Selecting a model to predict the onset of growth of *Fagus sylvatica*. Journal of Applied Ecology 31:172–181.

Kreyling, J. 2010. Winter climate change: a critical factor for temperate vegetation performance. Ecology 91:1939–1948.

Landsberg, J. J. 1974. Apple fruit bud development and growth; analysis and an empirical model. Annals of Botany 38:1013–1023.

Lavender, D. P. 1991. Measuring phenology and dormancy. Pages 403–422 *in* J. P. Lassoie and T. M. Hinkley, editors. Techniques and Methodologies in Tree Ecophysiology. CRC Press, Boca Raton, FL.

Lawler, J. J. 2009. Climate change adaptation strategies for resource management and conservation planning. Annals of the New York Academy of Sciences 1162:79–98.

Lenoir, J., T. Hattab, and G. Pierre. 2017. Climatic microrefugia under anthropogenic climate change: implications for species redistribution. Ecography 40:253–266.

Lockhart, J. A. 1983. Optimum growth initiation time for shoot buds of deciduous plants in a temperate climate. Oecologia 60:34–37.

Lookingbill, T. R., and D. L. Urban. 2003. Spatial estimation of air temperature differences for landscape-scale studies in montane environments. Agricultural and Forest Meteorology 114:141–151.

Luoto, M., and R. K. Heikkinen. 2008. Disregarding topographical heterogeneity biases species turnover assessments based on bioclimatic models. Global Change Biology 14:483–494.

Lute, A. C., J. T. Abatzoglou, and K. C. Hegewisch. 2015. Projected changes in snowfall extremes and interannual variability of snowfall in the western United States. Water Resources Research 51:960–972.

Menzel, A., T. H. Sparks, N. Estrella, E. Koch, A. Aasa, R. Ahas, K. Alm-Kübler, P. Bissolli, O. Braslavská, A. Briede, F. M. Chmielewski, Z. Crepinsek, Y. Curnel, Å. Dahl, C. Defila, A. Donnelly, Y. Filella, K. Jatczak, F. Måge, A. Mestre, Ø. Nordli, J. Peñuelas, P. Pirinen, V. Remišová, H. Scheifinger, M. Striz, A. Susnik, A. J. H. Van Vliet, F.-E. Wielgolaski, S. Zach, and A. Zust. 2006. European phenological response to climate change matches the warming pattern. Global Change Biology 12:1969–1976.

Morelli, T. L., C. Daly, S. Z. Dobrowski, D. M. Dulen, J. L. Ebersole, S. T. Jackson, J. D. Lundquist, C. I. Millar, S. P. Maher, W. B. Monahan, K. R. Nydick, K. T. Redmond, S. C. Sawyer, S. Stock, and S. R. Beissinger. 2016. Managing climate change refugia for climate adaptation. PLOS ONE 11:e0159909.

Mote, P. W. 2006. Climate-driven variability and trends in mountain snowpack in western North America. Journal of Climate 19:6209–6220.

Mote, P. W., S. Li, D. P. Lettenmaier, M. Xiao, and R. Engel. 2018. Dramatic declines in snowpack in the western US. Climate and Atmospheric Science 1:2.

Mote, P. W., and E. P. Salathe Jr. 2010. Future climate in the Pacific Northwest. Climatic Change 102:29–50.

Murray, M. B., M. G. R. Cannell, and R. I. Smith. 1989. Date of budburst of fifteen tree species in Britain following climatic warming. Journal of Applied Ecology 26:693–700.

Novick, K. A., A. C. Oishi, and C. F. Miniat. 2016. Cold air drainage flows subsidize montane valley ecosystem productivity. Global Change Biology 22:4014–4027.

Parmesan, C. 2006. Ecological and evolutionary responses to recent climate change. Annual Review of Ecology, Evolution, and Systematics 37:637–669.

Parmesan, C., and G. Yohe. 2003. A globally coherent fingerprint of climate change impacts across natural systems. Nature 421:37–42.

Pepin, N. C., C. Daly, and J. Lundquist. 2011. The influence of surface versus free-air decoupling on temperature trend patterns in the western United States. Journal of Geophysical Research: Atmospheres 116:D10109.

Perry, T. O. 1971. Dormancy of trees in winter. Science 171:29–36.

Peterson, D. L., E. G. Schreiner, and N. M. Buckingham. 1997. Gradients, vegetation and climate: spatial and temporal dynamics in the Olympic Mountains, U.S.A. Global Ecology and Biogeography Letters 6:7–17.

Polgar, C. A., and R. B. Primack. 2011. Leaf-out phenology of temperate woody plants: from trees to ecosystems. New Phytologist 191:926–941.

Potter, K. A., A. H. Woods, and S. Pincebourde. 2013. Microclimatic challenges in global change biology. Global Change Biology 19:2932–2939.

Rathcke, B., and E. P. Lacey. 1985. Phenological patterns of terrestrial plants. Annual Review of Ecology and Systematics 16:179–214.

Reed, B. C., M. White, and J. F. Brown. 2003. Remote sensing phenology. Pages 365–381 Phenology: An Integrative Environmental Science. Springer, Dordrecht.

Saxe, H., M. G. R. Cannell, Ø. Johnsen, M. G. Ryan, and G. Vourlitis. 2001. Tree and forest functioning in response to global warming. New Phytologist 149:369–399.

Schulze, M. 2017. Vegetative Phenology observations at the Andrews Experimental Forest, 2009 - Present.

Schulze, M., and A. Levno. 2017. Snow depth and snow water equivalent measurements along a road course and historic snow course in the Andrews Experimental Forest, 1978 to present.

Spies, T. 2015. Aboveground live biomass (2008), Andrews Experimental Forest.

Spies, T. 2016. Spies, T. 2016. LiDAR data (August 2008) for the Andrews Experimental Forest and Willamette National Forest study areas.

Spies, T. A., J. F. Franklin, and M. Klopsch. 1990. Canopy gaps in Douglas-fir forests of the Cascade Mountains. Canadian Journal of Forest Research 20:649–658.

Sproles, E. A., A. W. Nolin, K. Rittger, and T. H. Painter. 2013. Climate change impacts on maritime mountain snowpack in the Oregon Cascades. Hydrology and Earth System Sciences 17:2581–2597.

Sproles, E. A., T. R. Roth, and A. W. Nolin. 2017. Future snow? A spatial-probabilistic assessment of the extraordinarily low snowpacks of 2014 and 2015 in the Oregon Cascades. The Cryosphere; Katlenburg-Lindau 11:331–341.

Thackeray, S. J., P. A. Henrys, D. Hemming, J. R. Bell, M. S. Botham, S. Burthe, P. Helaouet, D. G. Johns, I. D. Jones, D. I. Leech, E. B. Mackay, D. Massimino, S. Atkinson, P. J. Bacon, T. M. Brereton, L. Carvalho, T. H. Clutton-Brock, C.

Duck, M. Edwards, J. M. Elliott, S. J. G. Hall, R. Harrington, J. W. Pearce-Higgins, T. T. Høye, L. E. B. Kruuk, J. M. Pemberton, T. H. Sparks, P. M. Thompson, I. White, I. J. Winfield, and S. Wanless. 2016. Phenological sensitivity to climate across taxa and trophic levels. Nature 535:241–245.

Valentine, T., and T. DeSilva. 2014. Adminstrative boundary, Andrews Experimental Forest, 1997 survey, 2009 update.

Valentine, T., and G. Lienkaemper. 2005. 30 meter digital elevation model (DEM) clipped to the Andrews Experimental Forest, 1996.

Visser, M. E., and C. Both. 2005. Shifts in phenology due to global climate change: the need for a yardstick. Proceedings of the Royal Society of London B: Biological Sciences 272:2561–2569.

Visser, M. E., C. Both, and M. M. Lambrechts. 2004. Global climate change leads to mistimed avian reproduction. Pages 89–110 *in* B.-A. in E. Research, editor. Birds and Climate Change. Academic Press.

Vitasse, Y., C. Signarbieux, and Y. H. Fu. 2018. Global warming leads to more uniform spring phenology across elevations. Proceedings of the National Academy of Sciences 115:1004–1008.

Walther, G.-R., E. Post, P. Convey, A. Menzel, C. Parmesan, T. J. C. Beebee, J.-M. Fromentin, O. Hoegh-Guldberg, and F. Bairlein. 2002. Ecological responses to recent climate change. Nature 416:389–395.